EXPERIMENTAL STUDY OF HOLOGRAPHY WITH PARTIALLY COHERENT LIGHT

部份諧后光之全息實驗研究

A Thesis

Submitted to

The Graduate School of

The Chinese University of Hong Kong

(Division of Physics)

In Partial Fulfillment

of the Requirements for the Degree of

Master of Philosophy in Physics

by

NG Yin-mui

吳燕梅

May 1976

ACKNOWLEDGEMENTS

I would like to express my sincere gratitude to my supervisor, Mr. L.K. Su, for his valuable advice and encouragement during this work. I would also like to thank Dr. S.T. Hsue of the University of Northern Iowa for his patient guidance in the basic techniques in Holography. The helpful suggestions and comments by Dr. S.Y. Feng and Dr. H.M. Lai are gratefully acknowledged. I also wish to thank my friend Mr. C.W. Kung for his help in the preparation of this thesis.

The financial support of the Institute of Science and Technology of the Chinese University of Hong Kong is cordially acknowledged.

CONTENTS

LIST OF FIGURES

ABSTRACT

Holograms recorded with coherent light and reconstructed with both coherent and partially coherent light were studied experimentally in this work.

Only tramission holograms recorded with lensless Fourier transform method were studied in this work in order to simplify the mathematical calculation. A small hole was made just underneath the subject letters on the subject transparency to let through the incident light directly, so that three-beam (two reference beams and one subject beam) interference pattern was recorded nonlinearly on the photographic plate. After we made a hologram with He-Ne laser, images were reconstructed with point illuminating source from a high pressure mercury lamp or an incandesent light from a projector. In reconstruction with incoherent light, achromatic images free of image blur from color dispersions were observed at the location of central zero-order, whilst color dispersions appeared at the first and higher diffraction orders. The reconstruction was also done with He-Ne laser as the illuminating source. The images could be reconstructed from the zero up to the third diffraction order. Thus it provides a good method to exhibit the high order Fourier transform images.

CHAPTER 1

INTRODUCTION

A coherent light source is usually used for both the hologram recording and wavefront reconstruction. In some cases, the use of incoherent white light source for reconstruction is desirable, especially for display.

After recording by coherent light, the reconstructed images of holograms by incoherent white light suffer the color blurring from dispersion by the spectral width (the lack of temporal coherence) and the extended size of the reconstructing light source (the lack of spatial coherence). [Appendix I] It was shown by Yasuhiro Torii and Masao Sumi (1971) [8] that the distortion of the reconstructed image depending on the wavelength ratio of reconstructing to recording light is negligible, thus the reconstructed images by incoherent light are blurred especially by color dispersion for the light source with broad spectral width.

It is well known that there are the Lippmann-Bragg type hologram [Appendix II] and the focussed-image hologram [Appendix III] which are not much affected by color dispersion. [1, 2, 3, 4] Besides these two types, there is another method of dispersion compensation to give the bright achromatic images by the white light reconstruction.

In 1966, C.B. Burckhardt reported that coherently recorded hologram can be reconstructed with white light source [6] . The diffracted beam of the hologram is diffracted a second time at a

plane transmission grating which can be formed photographically with two plane waves. This compensating grating produces an equal but opposite dispersion to the hologram diffraction. Thus the large color dispersion at the hologram is compensated by the grating since the light is diffracted in the opposite direction. As a consequence of the double diffraction, the reconstructed achromatic wave appears in the direction of the illuminating wave. The double diffraction is shown schematically in Fig. 1.1 .

Nearly at the same time, D.J. De Bitetto also reported that priams or a single-plane diffraction grating can be used as the correcting element for dispersion compensation for achromatizing the white-light reconstruction [7]. The theory of using a single-plane diffraction grating as the correcting element is the same as that explained by Burckhardt.

A few years later, Yasuhiro Torii and Masao Sumi derived in detail the generalized formula for the reconstructed image by incoherent light and the degree of the improvement for the achromatized reconstructed images with the diffraction grating for compensating color dispersion[8]. The image blur from color dispersion and by the reconstructing light source size are also discussed. Distortion of the reconstructed images depending on the wavelength ratio of reconstructing to recording light is shown to be negligible. All these characteristics of holograms reconstructed by incoherent light were demonstrated experimentally [9].

However, the correcting element for dispersion compensation in the previous experiments is a plane-transmission diffraction grating which is separated from the original hologram. Thus two holograms are

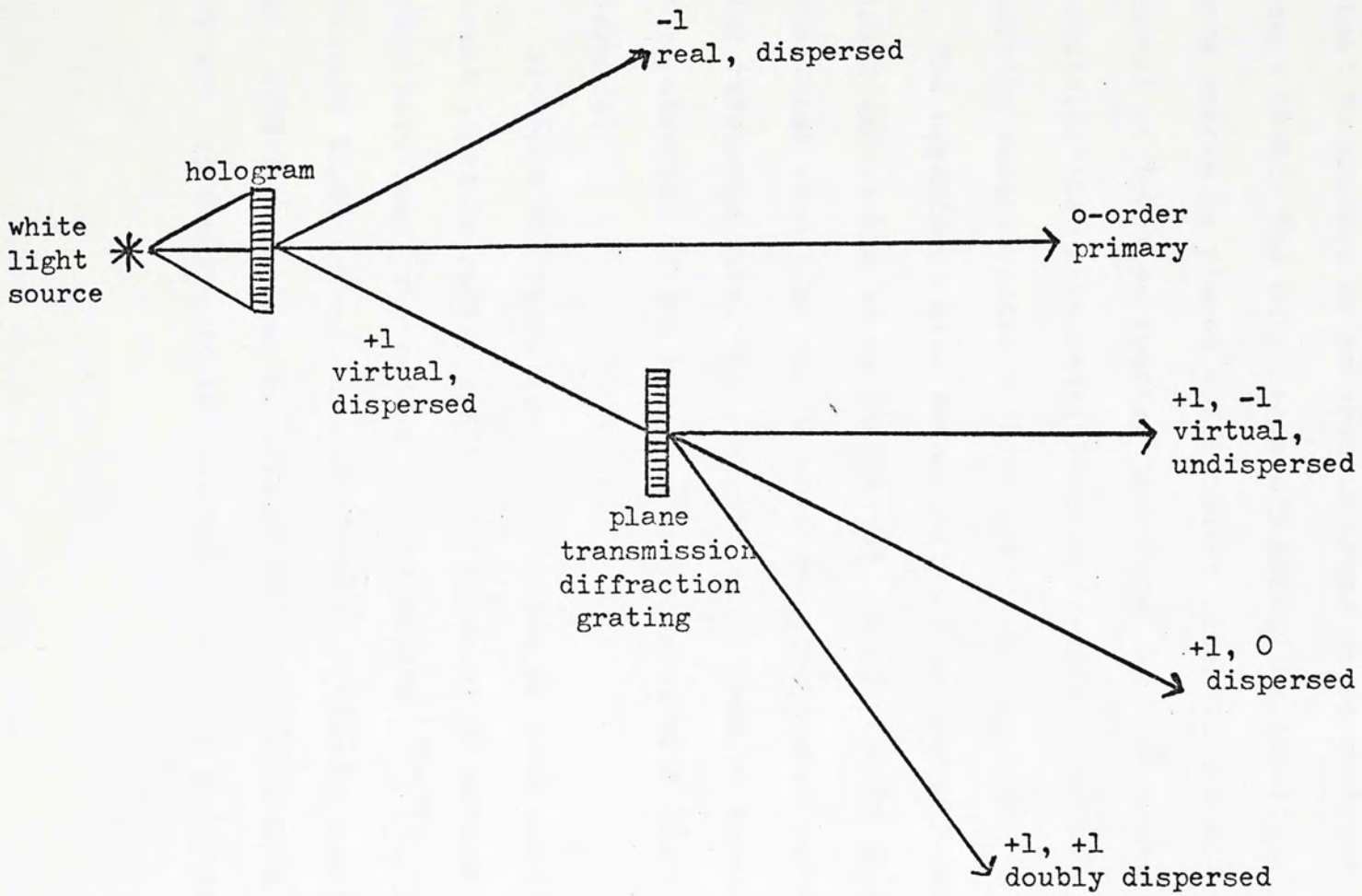

Fig. 1.1 Schematic diagram of the arrangement for achromatizing the white-light reconstruction wave by a plane transmission diffraction grating

needed in reconstruction with incoherent light source, and in addition, it is also necessary to decide their separation and relative positions. A new method is discussed in this thesis in which a single hologram is sufficient to produce an achromatic image on reconstruction with incoherent light. The only necessary recording condition is that the reference source is placed sufficiently close to the subject in the arrangement of lensless Fourier transform. We have demonstrated experimentally that achromatic Fourier transform images can be successfully reconstructed with this method.

The experiment also demonstrates that images located at zero and higher orders can be reconstructed simultaneously when the hologram is a nonlinear record of the three-beam interference pattern with an addition reference wave. Those higher order Fourier transform images cannot be observed if the hologram is recorded with two-beam interference.

Although the formation of holograms of good quality by incoherent light is rather difficult, a number of methods for forming holograms have been proposed in the literature [26-35]. In experiments with mercury light source, an interference filter is usually added. However, efforts have been made to record a hologram with unfiltered mercury arc and the result is reported briefly in Appendix IV.

CHAPTER 2

THEORY

The theory is derived under the assumptions

(1) all illumination in the recording process is perfectly coherent

(2) the holograms behave as plane diffraction gratings.

In this chapter, from Section 2.1 to Section 2.4 are reviews of the basic theory, whilst Section 2.5 and Section 2.6 are derivation of the three-beam interference holographic theory base on the two-beam interference holographic theory.

2.1 GENERAL DESCRIPTION

Electromagnetic wave at optical wavelengths can be spatially modulated and may be analyzed in either a spatial domain or a spatial frequency domain. In the spatial domain the light complex amplitude $a(x,y)$ is expressed as a function of the x, y spatial co-ordinates of an observation plane through which the light propagates. The same complex amplitude distributions can be expressed in terms of orthogonal spatial frequencies ξ and η as well. According to the basic theorems of Fourier analysis, as applied to light distributions, any two-dimensional complex amplitude pattern can be considered as a discrete or continuous set of sinusoidally varying patterns (periodic components). The reciprocal of the spatial period of any of the components of the set, measured in a given direction on the observation plane, is called the spatial frequency of that component in the assigned direction. By resolving spatial periods into two

orthogonal components along the x and y directions we can obtain the corresponding spatial frequency components ξ and η . Thus the light complex amplitude distribution a(x,y) in the spatial domain may be expressed as another function A (ξ,η) in the spatial frequency domain. The function A(ξ , η) is given by Fourier transform of a(x,y), F [a(x,y)] , where

$$F[a(x,y)] = A(\xi,\eta) = \int_{-\infty}^{\infty}\int_{-\infty}^{\infty} a(x,y)\exp(2\pi i\xi x)\exp(2\pi i\eta y)dxdy$$

or represented symbolically as

$$a(x,y) \supset A(\xi,\eta)$$

Conversely, a(x,y) is given by the inverse Fourier transform of A(ξ , η) such that

$$F^{-1}[A(\xi,\eta)] = a(x,y) = \int_{-\infty}^{\infty}\int_{-\infty}^{\infty} A(\xi,\eta)\exp(-2\pi i\xi x)\exp(-2\pi i\eta y)d\xi\, d\eta$$

or represented symbolically as

$$A(\xi,\eta) \subset a(x,y)$$

Thus in the optical system, the Fourier transformation can be regarded as a decomposition of a general light wave into many plane waves whose direction cosines correspond to the spatial frequencies.

2.2 COMPUTATION OF SUBJECT AND REFERENCE PHASE AT ANY POINT ON THE HOLOGRAM PLANE

In the analysis to follow, a subject or reference wave arriving at any point Q on the hologram plane (Fig. 2.1) is to be represented by the difference in its phase at Q over the phase at a fixed point 0.

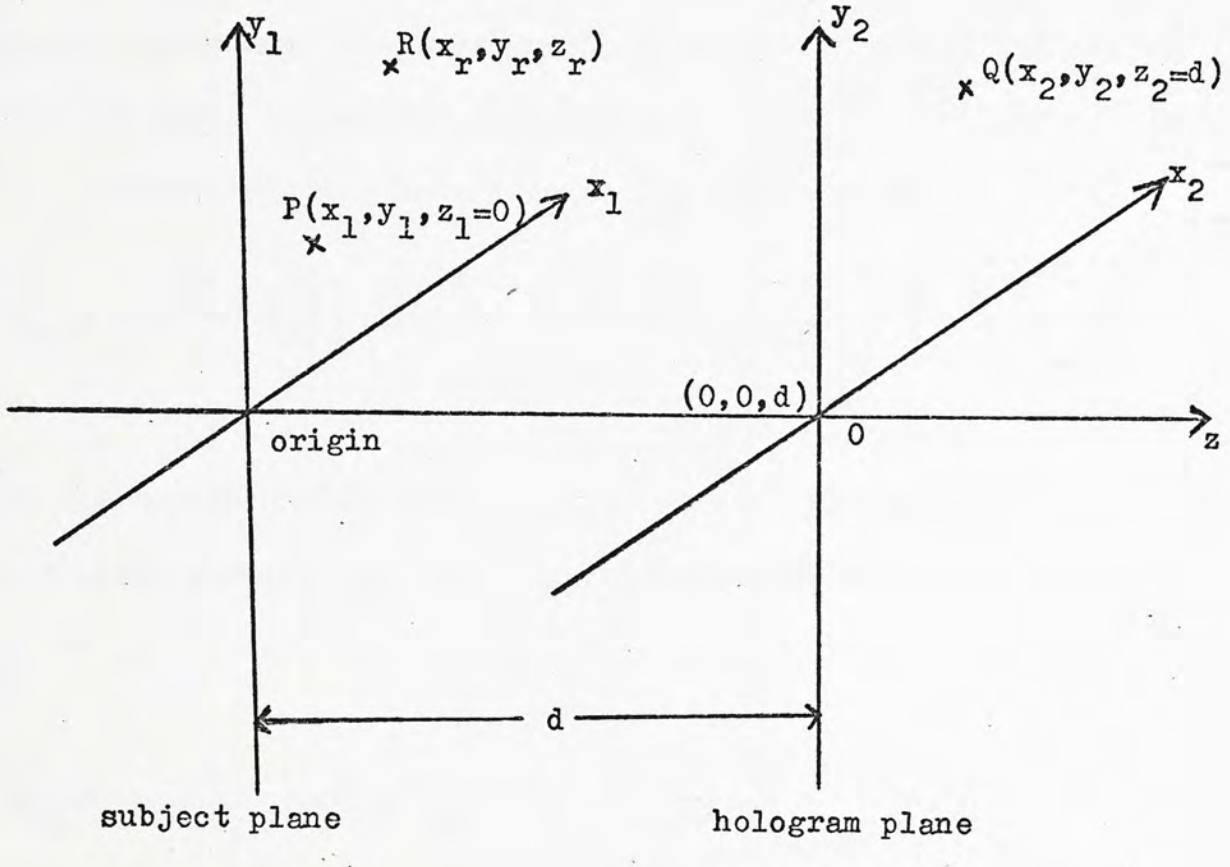

Fig. 2.1 Parameters required for computation of φ_a and φ_r

Consider now hologram formation as indicated in Fig. 2.1. The subject point source P is in the x_1y_1 plane. The fixed point 0 is located at the centre of the hologram x_2y_2 plane. z_2 = d units from the subject plane. A reference point source R is located in some arbitrary plane x_ry_r , a distance z_r from the subject plane.

Let $a = a_o \exp(i\,\varphi_a)$ be the complex amplitude of the light arriving at any point on the hologram plane from the subject point source and let $r = r_o \exp(i\,\varphi_r)$ be the complex amplitude of the reference wave at the hologram plane. Then the phase of the subject wave at Q, $\varphi_a(x,y)$, is given by

$$\varphi_a = \frac{-2\pi}{\lambda} (PQ - PO)$$

where λ represents the wavelength, and the minus sign represents diverging light is emitted from the point source.

Substitute the co-ordinates of P,Q,O, we get

$$\varphi_a = - \frac{2\pi}{\lambda} z_2 \left\{ \left[1 + \frac{(x_2-x_1)^2 + (y_2-y_1)^2}{z_2^2} \right]^{\frac{1}{2}} - \left[1 + \frac{x_1^2+y_1^2}{z_2^2} \right]^{\frac{1}{2}} \right\}$$

with the approximation that P and Q are not far off the z-axis, and if z_2 is large enough, φ_a can be approximated to the first order in $\frac{1}{z_2}$ by

$$\varphi_a \cong - \frac{\pi}{\lambda z_2} (x_2^2 + y_2^2 - 2x_2x_1 - 2y_2y_1)$$

Similarly, the reference phase at Q, $\varphi_r(x_2,y_2)$, is

$$\varphi_r \cong - \frac{\pi}{\lambda z_2} (x_2^2 + y_2^2 - 2x_2x_r - 2y_2y_r) \qquad (2.1)$$

assuming $z_2 \gg z_r$

2.3 ACHROMATIC IMAGES RECONSTRUCTED WTIH LENSLESS FOURIER TRANSFORM HOLOGRAM

The subject transparency of transmittance $s(x_1,y_1)$ is placed in the x_1y_1 plane at a distance d from the hologram plane (x_2y_2 plane) as shown in Fig. 2.2 , and illuminated by an incident plane wave of constant amplitude a_1.

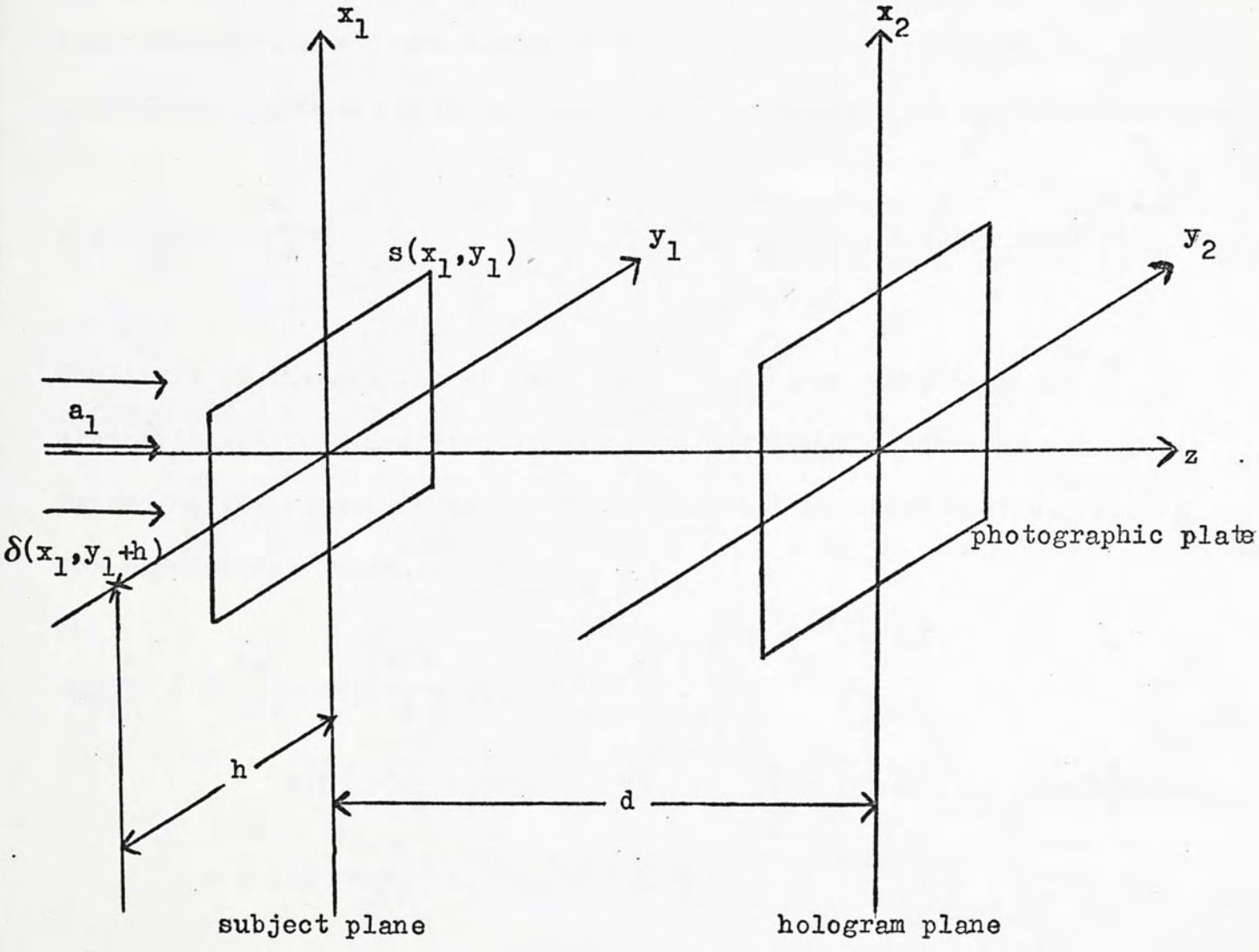

Fig. 2.2 Recording of the Lensless Fourier transform Hologram

The reference point source $\delta(x_1, y_1+h)$ is in the subject plane and displaced -h units in y_1 axis from the centre of the subject transparency. Then the subject wavefront to be recorded at the hologram plane is the near-field or Fresnel diffraction pattern of the subject transparency.

According to Fresnel-Kirchhoff integral [Appendix V], with the approximation that $(x_2-x_1) << d$ and $(y_2-y_1) << d$, the complex amplitude of the subject light in the x_2y_2 hologram plane can be written as following, with a factor constant over the plane $z_2=d$ has been neglected.

$$a(x_2,y_2) = \frac{ia_1}{\lambda d}\int_{x_1=-\infty}^{\infty}\int_{y_1=-\infty}^{\infty} s(x_1,y_1)\exp\left\{\frac{-i\pi}{\lambda d}\left[(x_2-x_1)^2+(y_2-y_1)^2\right]\right\}dx_1dy_1$$

The limit of integration extends from $-\infty$ to $+\infty$ providing the transmittance function $s(x_1,y_1)$ is zero outside the transparency area. Expanding the square terms in the exponential function and rearranging the exponential function, we get

$$\begin{aligned} a(x_2,y_2) &= \frac{ia_1}{\lambda d}\exp\left\{\frac{-i\pi}{\lambda d}(x_2^2+y_2^2)\right\} \\ &\quad \times \iint s(x_1,y_1)\exp\left[\frac{-i\pi}{\lambda d}(x_1^2+y_1^2)\right]\exp\left[2\pi i(\xi x_1+\eta y_1)\right]dx_1dy_1 \\ &= c\exp\left\{\frac{-i\pi}{\lambda d}\left[(x_2^2+y_2^2)\right]\right\}S(\xi,\eta) \qquad (2.2) \end{aligned}$$

where a_1 = amplitude of the incident plane wave

$c = \frac{ia_1}{\lambda d}$ is a complex number

$\xi = \frac{x_2}{\lambda d}$ spatial frequency in x-direction in x_1y_1 plane

$\eta = \frac{y_2}{\lambda d}$ spatial frequency in y-direction in x_1y_1 plane

$$S(\xi, \eta) \subset s(x_1, y_1) \exp\left[\frac{-i\pi}{\lambda d}(x_1^2+y_1^2)\right]$$

Complex amplitude of the spherical reference wave at the hologram plane is

$$R(x_2, y_2) = r_o \exp(i\varphi_R)$$

where φ_R is given by Eq.(2.1) with $z_2 = d$, $x_r = 0$ and $y_r = -h$.

Then the reference wave is given by

$$R(x_2, y_2) = r_o \exp\left[\frac{-i\pi}{\lambda d}(x_2^2+y_2^2)\right] \exp\left[-2i\pi\eta h\right] \qquad (2.3)$$

Interference between R and a produces a pattern on the photographic plate whose intensity is

$$I = (a+R)(a+R)^* = aa^* + RR^* + aR^* + a^*R$$

where a+R is the total complex amplitude on the photographic plate and * represents its complex conjugate.

After the usual dark-room processing, the photographic plate becomes a hologram . We assume the developed hologram has a transmittance $t(x,y) \propto I$ if the hologram is recorded linearly.

The image forming terms of the hologram transmittance are given by

$$aR^* + a^*R = cr_oS(\xi, \eta)\exp(2\pi i\eta h) + c^*r_oS^*(\xi, \eta)\exp(-2\pi i\eta h)$$

If the hologram is illuminated with a plane wave propagating along the z-axis with constant amplitude r_o, the product $r_o t(x,y)$ represents the complex amplitude u of the diffracted light just behind the hologram, where

$$u \propto r_o t(x,y)$$

$$\propto I = |a|^2 + r_o^2 + c r_o S(\xi;\eta)\exp(2\pi i \eta h) + c^* r_o S^*(\xi,\eta)\exp(-2\pi i \eta h) \tag{2.4}$$

A lens placed immediately before or after the hologram will display in its back focal plane the product of the inverse Fourier transform of u and a spherical phase factor. If we detect only the intensity in the back focal plane then we can neglect the spherical phase factor.

The zero order term of Eq. (2.4), $|a|^2 + r_o^2$, will be focused about the origin of image plane as shown in Fig. 2.3 .

The inverse Fourier transform of the third term of Eq.(2.4) is given by

$$\begin{aligned} & c r_o \iint S(\xi,\eta)\exp(2\pi i \eta h)\exp[-2\pi i(\xi x_3 + \eta y_3)]\, d\xi\, d\eta \\ = \; & c r_o \iint \left\{ \iint s(x_1,y_1)\exp\left[\frac{-i\pi}{\lambda d}(x_1^2+y_1^2)\right]\exp\left[2\pi i(\xi x_1 + \eta y_1)\right] dx_1 dy_1 \right\} \\ & \quad \times \left\{ \exp(2\pi i \eta h)\exp\left[-2\pi i(\xi x_3 + \eta y_3)\right] \right\} d\xi\, d\eta \\ = \; & c r_o s(x_3, y_3 - h)\exp\left\{\frac{-i\pi}{\lambda d}\left[x_3^2 + (y_3-h)^2\right]\right\} \end{aligned} \tag{2.5}$$

this is the original transmittance times a spherical phase factor shifted h units from the origin in the positive y-axis in the $x_3 y_3$ image plane.

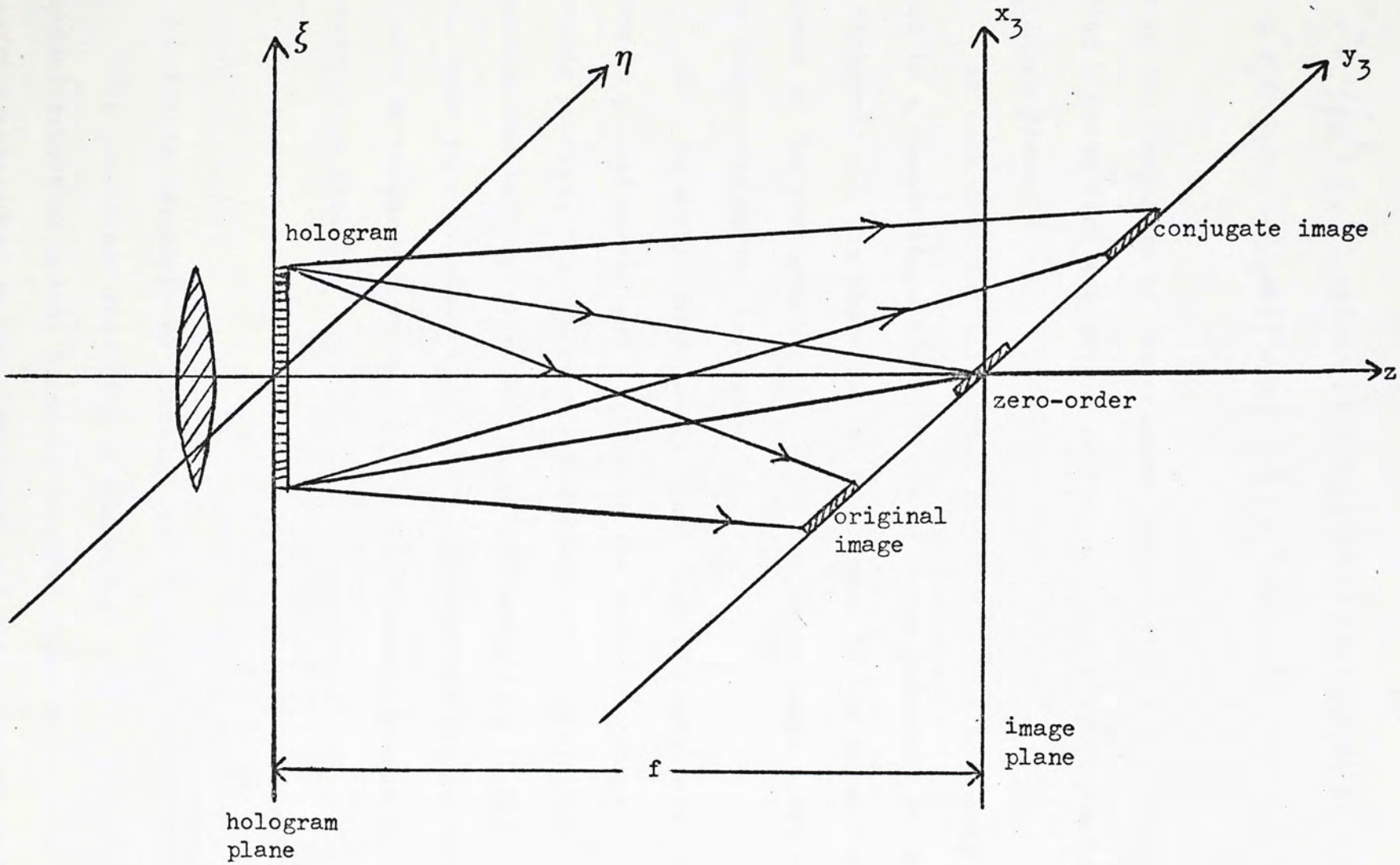

Fig. 2.3 Generation of two real images from a Fourier transform hologram

The inverse Fourier transform of the fourth term yields

$$c^* r_o \iint S^*(\xi,\eta)\exp(-2\pi i \eta h)\exp[-2\pi i(\xi x_3+\eta y_3)]\, d\xi\, d\eta$$

$$= c^* r_o S^*[-x_3, -(y_3+h)] \exp\left\{\frac{i\pi}{\lambda d}[x_3^2+(y_3+h)^2]\right\} \qquad (2.6)$$

this is the conjugate of the original transmittance, inverted and shifted h units from the origin in the negative y-direction in the x_3y_3 image plane.

In each case the diffracted light converges to a real image formed in a common image plane. Since only the intensity of the images are observed, all the phase factor drops out. If the intensity is detected by the photographic film, the conjugate image differs from the other image only by its inversion.

If h is sufficiently small, such that the reference point source is placed sufficiently close to the subject transparency in the recording process, the images reconstructed will suffer less dispersion and be very close to the zeroth order term in the image plane. Thus these two images will be achromatic and can be observed even with an incoherent white light as illuminating source in the reconstruction process.

2.4 NON-LINEAR RECORDING OF LENSLESS FOURIER TRANSFORM HOLOGRAM

The non-linear recording of the signal wave is the most important source of noise. Noise is unwanted light which is not linearly proportional to the signal wave and diffracted or scattered

from the hologram in the same general direction as the reconstructed wave.

In recording a hologram, we generally assume a linear relation between the amplitude transmittance t and exposure E of the hologram, that is given by

$$t = t_o - KI \tag{2.7}$$

where t_o = the transmittance of the unexposed (but developed) photographic plate

K = constant

I = intensity of the interference pattern and $I \propto E$

The t-E curves of actual recording media are always nonlinear to some degree [Appendix VI]. If the range of exposure fluctuations given by

$$E_o(1-V_{max}) < E < E_o(1+V_{max})$$

where E_o = average exposure

V_{max} = the maximum fringe visibility in the exposing interference pattern

is kept within the linear portion of the t-E curve, adverse effects on image quality will be minimized and the transmittance of the hologram is given by Eq.(2.7).

The general form of the amplitude transmittance of a hologram is

$$t = c_o + c_1E + c_2E^2 + c_3E^3 \tag{2.8}$$

where $E \propto I$

For the usual range of exposure, nonlinear effects produced by the quadratic terms are the most important.

Assume the reference wave is unmodulated so that $rr^* =$ constant, then in Eq.(2.8), c_o is a constant, $c_1 E$ represents the linear relation, while $c_2 E^2 + c_3 E^3$ represent the nonlinear effect.

Consider the subject transparency of transmittance $s(x_1, y_1)$ is placed about the centre of the subject $x_1 y_1$ plane at a distance d from the hologram $x_2 y_2$ plane. The reference point source $\delta(x_1 + b, y_1)$ is in the subject plane and displaced -b units in x_1 axis from the centre of the subject transparency as shown in Fig 2.4 .

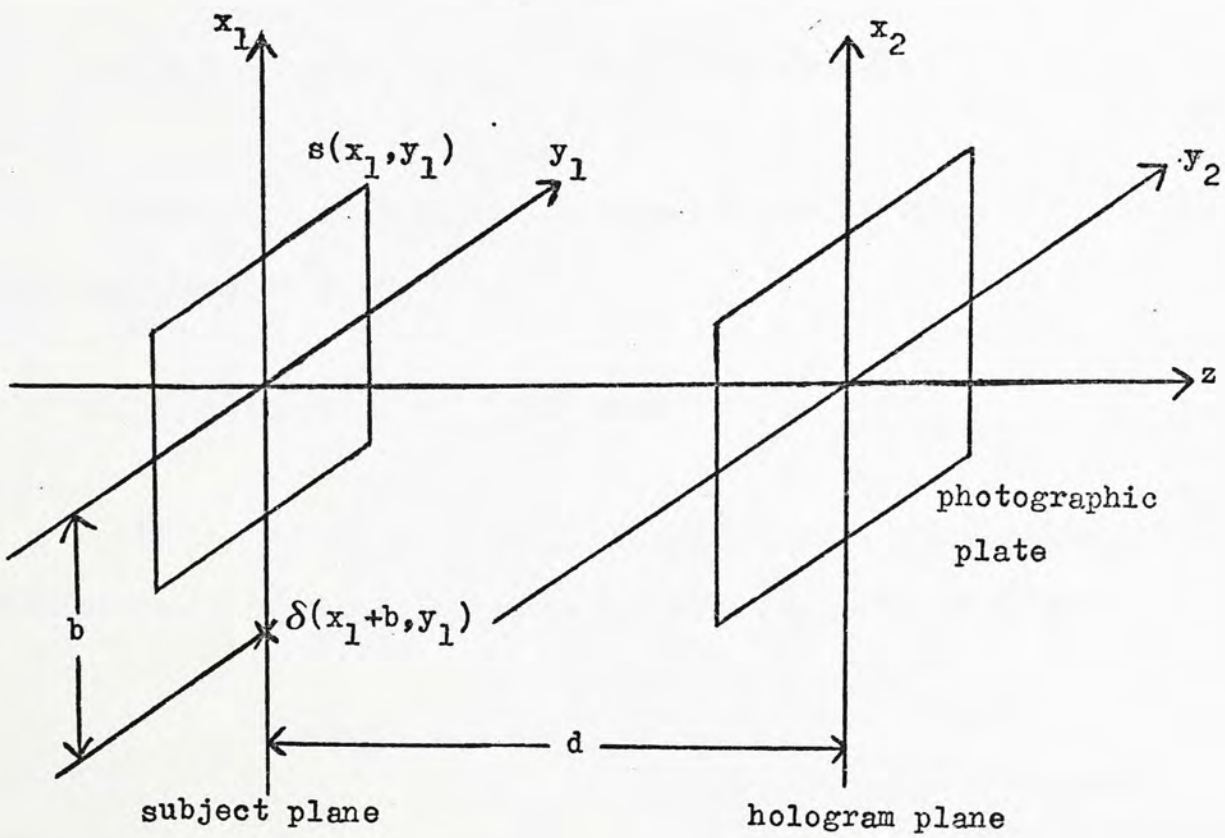

Fig. 2.4 Non-linear recording of the lensless Fourier transform hologram.

Complex amplitude of the subject wave on the x_2y_2 hologram plane is also given by Eq. (2.2)

$$a(x_2,y_2) = c \exp\left[\frac{-i\pi}{\lambda d}(x_2^2+y_2^2)\right] S(\xi,\eta)$$

Complex amplitude of the spherical reference wave at the hologram plane is

$$r(x_2,y_2) = r_o \exp(i\varphi_r)$$

where φ_r is given by Eq.(2.1) with $z_2 = d$, $x_r = -b$ and $y_r = 0$. Thus the reference wave is given by

$$r(x_2,y_2) = r_o \exp\left[\frac{-i\pi}{\lambda d}(x_2^2+y_2^2)\right] \exp\left[-2i\pi\xi b\right] \qquad (2.9)$$

Intensity of the interference pattern of these two waves on the hologram plane is given by

$$I = (a+r)(a+r)^* = r_o^2 + aa^* + ar^* + a^*r$$

If the hologram is recorded nonlinearly, the amplitude transmittance of the hologram is given by Eq.(2.8), such that

$$t = c_o + c_1 I + c_2 I^2 + c_3 I^3$$

The quadratic nonlinear effects are given by

$$I^2 = (r_o^2 + aa^* + ar^* + a^*r)^2$$

$$= r_o^4 + 2r_o^2 aa^* + aa^* aa^* + 2a^* rar^* + (2r_o^2 + 2aa^*)ar^*$$

$$+ (2r_o^2 + 2aa^*)a^* r + ar^* ar^* + a^* ra^* r$$

$$= K_1 + K_2 ar^* + K_2 a^* r + (ar^*)^2 + (a^* r)^2 \qquad (2.10)$$

where $K_1 = r_o^4 + 2r_o^2 aa^* + aa^* aa^* + 2a^* rar^*$

$K_2 = 2r_o^2 + 2aa^*$

This expression contains linear terms and squared terms. Since we are primarily interested in qualitative analysis, we can neglect the addition of linear terms in Eq.(2.8).

Plane wave illumination of the hologram requires a lens, as in Fig.2.4, to carry out the inverse Fourier transform of the hologram transmittance. Inverse Fourier transform of 2nd and 3rd terms in Eq.(2.10) are given by Eq.(2.5) and Eq.(2.6) with $x_3 \rightarrow y_3$ and $h \rightarrow b$ such that given by

$$cr_o\, s(x_3-b, y_3) \exp\left\{\frac{-i\pi}{\lambda d}\left[(x_3-b)^2 + y_3^2\right]\right\} \qquad (2.11)$$

and $$c^* r_o s^*\left[-(x_3+b), -y_3\right] \exp\left\{\frac{i\pi}{\lambda d}\left[(x_3+b)^2 + y_3^2\right]\right\} \qquad (2.12)$$

Inverse Fourier transform of the squared terms is very complicated. However, these squared terms are analyzed qualitatively to show the orientation of the reconstructed images produced by these terms.

$$(a r^*)^2 = c^2 r_o^2 \left[S(\xi, \eta)\right]^2 \exp(4\pi i \xi b)$$

this represents that the square of the subject information is located

at (2b,0) in the image plane. Similarly,

$$(a^{*}r)^2 = (c^{*})^2 r_o^{\,2} [S^{*}(\xi,\eta)]^2 \exp(-4\pi i \xi b)$$

represents that the square of the conjugate subject information is located at (-2b,0) in the image plane.

The cubic term in Eq.(2.8) produces transmittance terms such that some of which have the same form as Eq.(2.10).

$$I^3 = [K_1+K_2 ar^{*}+K_2 a^{*}r+(ar^{*})^2+(a^{*}r)^2][r_o^{\,2}+aa^{*}+a^{*}r+ar^{*}]$$

$$= [K_1+K_2 ar^{*}+K_2 a^{*}r+(ar^{*})^2+(a^{*}r)^2][K_o+a^{*}r+ar^{*}]$$

where $K_o = r_o^{\,2}+aa^{*}$

$$I^3 = K_oK_1+2K_2 ar^{*}a^{*}r+(K_oK_2+K_1+1)ar^{*}+(K_oK_2+K_1+1)a^{*}r$$

$$+(K_o+K_2)(ar^{*})^2+(K_o+K_2)(a^{*}r)^2+(ar^{*})^3+(a^{*}r)^3$$

$$= D_o+D_1 ar^{*}+D_1 a^{*}r+D_2(ar^{*})^2+D_2(a^{*}r)^2+(ar^{*})^3+(a^{*}r)^3 \qquad (2.13)$$

where $D_o = K_oK_1+2K_2 ar^{*}a^{*}r$

$D_1 = K_oK_2+K_1+1$

$D_2 = K_o+K_2$

Analyzing the cubic nonlinear terms in Eq.(2.13), we obtain

$$(ar^{*})^3 = c^3 r_o^{\,3} [S(\xi,\eta)]^3 \exp(6\pi i \xi b)$$

$$(a^{*}r)^3 = (c^{*})^3 r_o^{\,3} [S^{*}(\xi,\eta)]^3 \exp(-6\pi i \xi b)$$

The images reconstructed on the image plane if the hologram is recorded nonlinearly are shown schematically as in Fig.2.5. It is obviously that only the first order images can be observed when the hologram is recorded nonlinearly. Since the second and higher order images are proportional to a^2 or a^n , where n represents nth diffraction order, thus these higher orders are not really the reconstruction of the original subject, and can only be read out as the diffracted bright spots.

In Fig.2.5, the positions of the higher order terms

$F^{-1}[(a^*r)^2]$, $F^{-1}[(ar^*)^2]$, $F^{-1}[(ar^*)^3]$ and $F^{-1}[(a^*r)^3]$

are shown. However, these are the actual positions of those inverse Fourier transformations only if the subject is an ideal point source. In the general condition, the subject is a collection of point sources, thus intermodulation terms will be included in these inverse Fourier transformations and give rise to a blurring background of the 1st order images [10]. This blurring background is in fact false images of point sources that are not actually present on the subject.

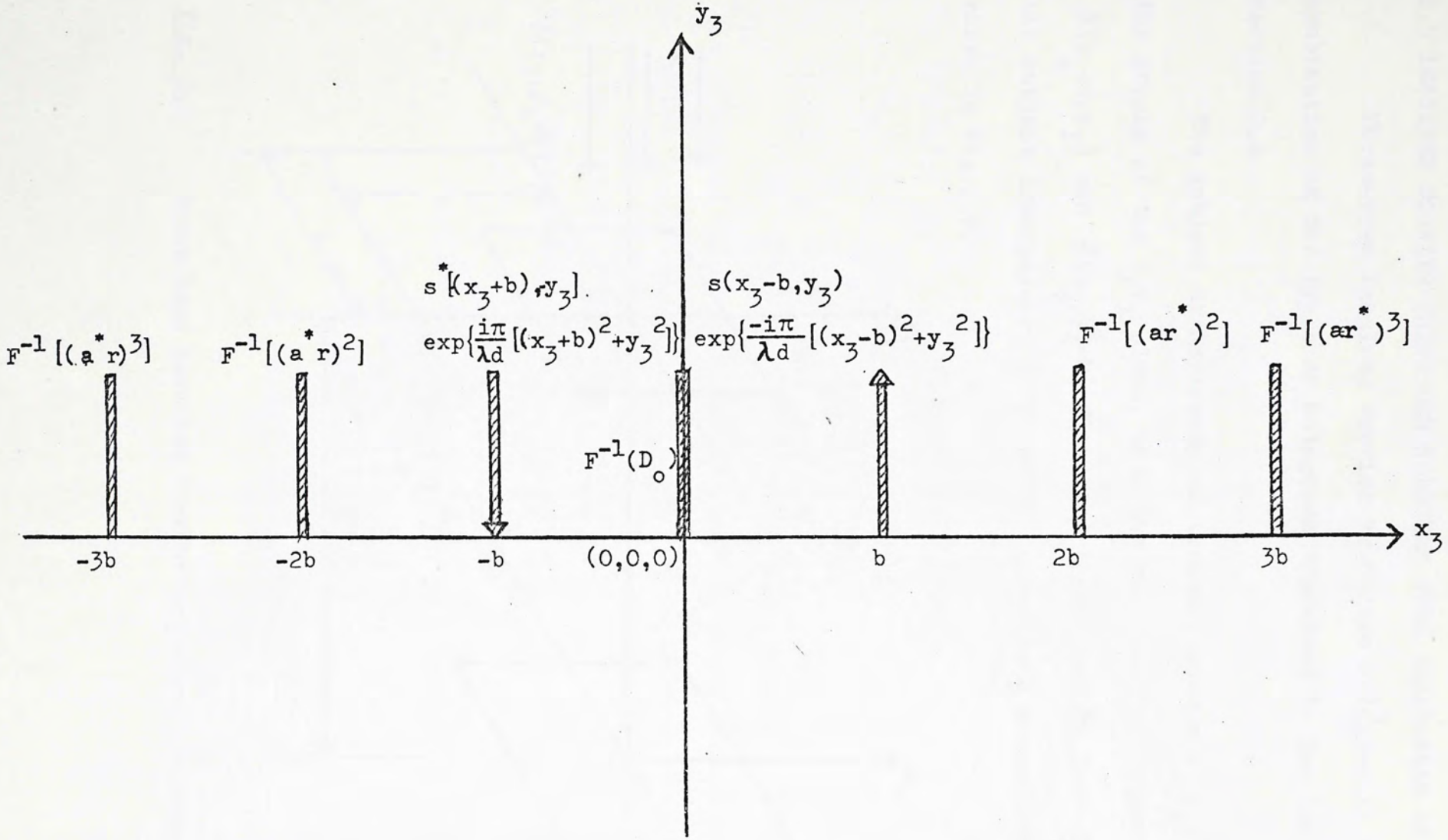

Fig. 2.5 Images reconstructed on image plane with nonlinearly recorded Fourier transform hologram

2.5 LENSLESS FOURIER TRANSFORM HOLOGRAM WITH THREE-BEAM INTERFERENCE

Three-beam lensless Fourier transform hologram is actually the combination of the types of holograms discussed in Section 2.3 and Section 2.4.

The subject transparency of transmittance $s(x_1,y_1)$ is placed at the origin of the x_1y_1 plane, with two reference point sources $\delta(x_1+b,y_1)$ and $\delta(x_1,y_1+h)$ displaced b and h units from the centre of the subject transparency in x_1 and y_1 directions respectively as shown in Fig.2.6.

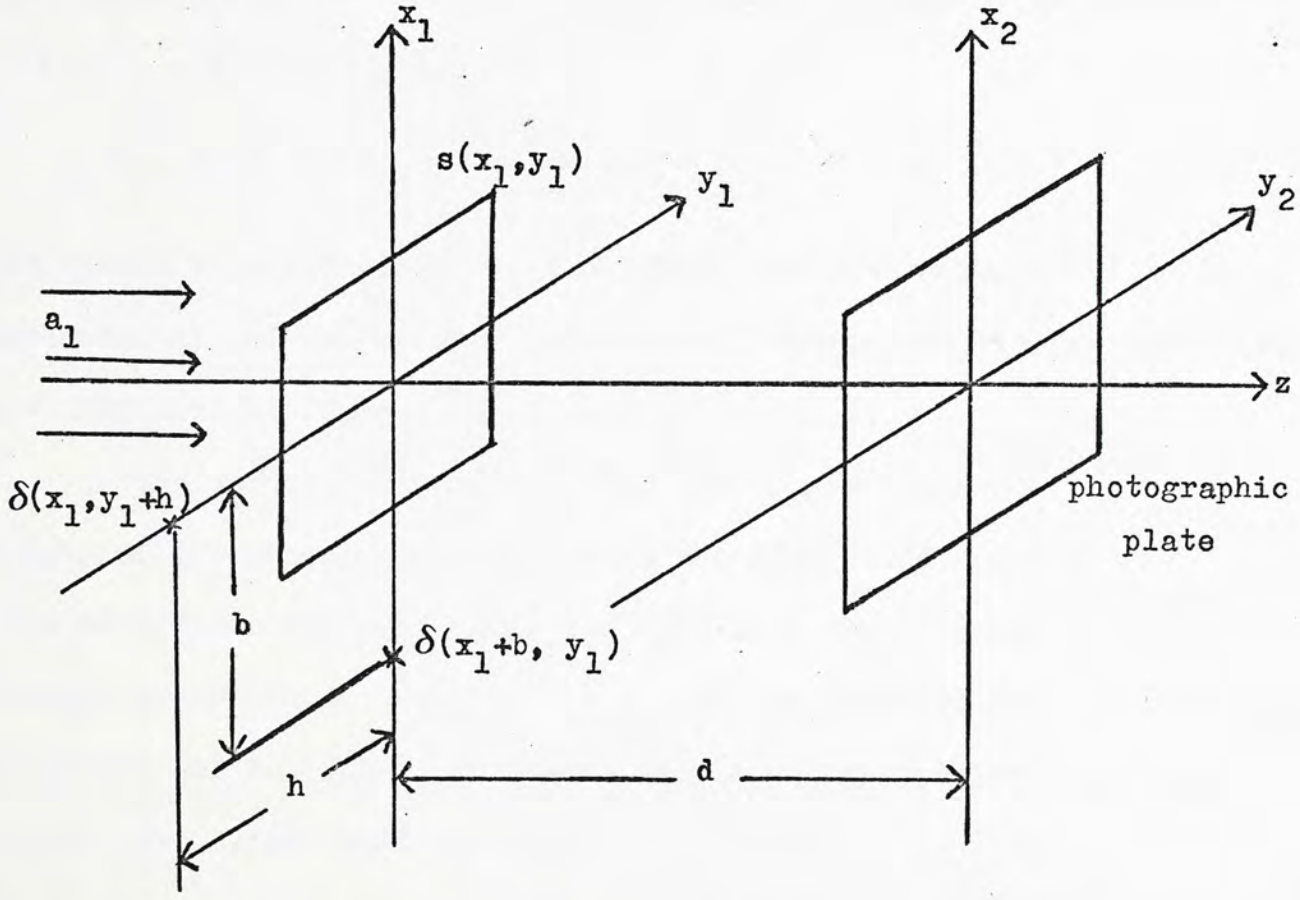

Fig. 2.6 Three-beam lensless Fourier transform hologram

Complex amplitudes of the subject beam and the two reference beams on the hologram plane are given by Eq.(2.2), Eq.(2.3) and Eq.(2.9) respectively. The photographic plate which is placed in the x_2y_2 plane at a distance d from the x_1y_1 subject plane records the three-beam interference pattern. The resultant complex amplitude on the hologram plane is

$$a(x_2,y_2) + R(x_2,y_2) + r(x_2,y_2)$$

The intensity of the three-beam interference pattern is given by

$$\begin{aligned} I &= (a + R + r)(a + R + r)^* \\ &= r_o^2 + aa^* + RR^* + r^*a + a^*r + r^*R + R^*r + aR^* + a^*R \end{aligned} \qquad (2.14)$$

with plane wave illumination, the images are reconstructed with the experimental set up as shown in Fig.2.3. The images reconstructed are actually inverse Fourier transforms of Eq.(2.14).

The zero-order terms, $r_o^2+aa^*+RR^*$, are focused about the origin of the image plane, and there are four first order images reconstructed corresponding to two reference light beams. Inverse Fourier transform of a^*r, ar^*, a^*R, aR^* as given by Eq.(2.5), Eq.(2.6), Eq.(2.11) and Eq.(2.12), indicates the location of these first order images. Two terms still remain to be analyzed,

$$\begin{aligned} &\iint r^* R \exp[-2\pi i(\xi x_3+\eta y_3)]\, d\xi\, d\eta \\ &= r_o^2 \iint \exp(2i\pi\xi b)\exp(-2i\pi\eta h)\exp[-2\pi i(\xi x_3+\eta y_3)]\, d\xi\, d\eta \\ &= r_o^2\, \delta(x_3-b,\ y_3+h) \end{aligned} \qquad (2.15)$$

$$\iint rR^{*} \exp\left[-2\pi i(\xi x_3+\eta y_3)\right] d\xi\, d\eta$$

$$= r_o^{2} \iint \exp(-2i\pi\xi b)\exp(2i\pi\eta h)\exp\left[-2\pi i(\xi x_3+\eta y_3)\right] d\xi\, d\eta$$

$$= r_o^{2}\ \delta(x_3+b, y_3-h) \qquad (2.16)$$

These two terms carry no subject information but only reconstruction of two bright spots. Locations of reconstructed images on the image plane are shown schematically in Fig.2.7 .

The result may be explained as following: two hologram diffraction gratings which are formed by interference of the subject wave and each reference wave respectively, and thus of mutually perpendicular orientations, are superimposed on the same photographic plate, so that the images reconstructed are two pairs of Fourier transform images located on two perpendicular axes. There is also an additional holographic diffraction grating formed by interference of the two reference waves which are originated from the two point sources located on two perpendicular axes in the same plane. Upon illumination by a plane wave, two bright points are reconstructed as the Fourier transform images of a point subject.

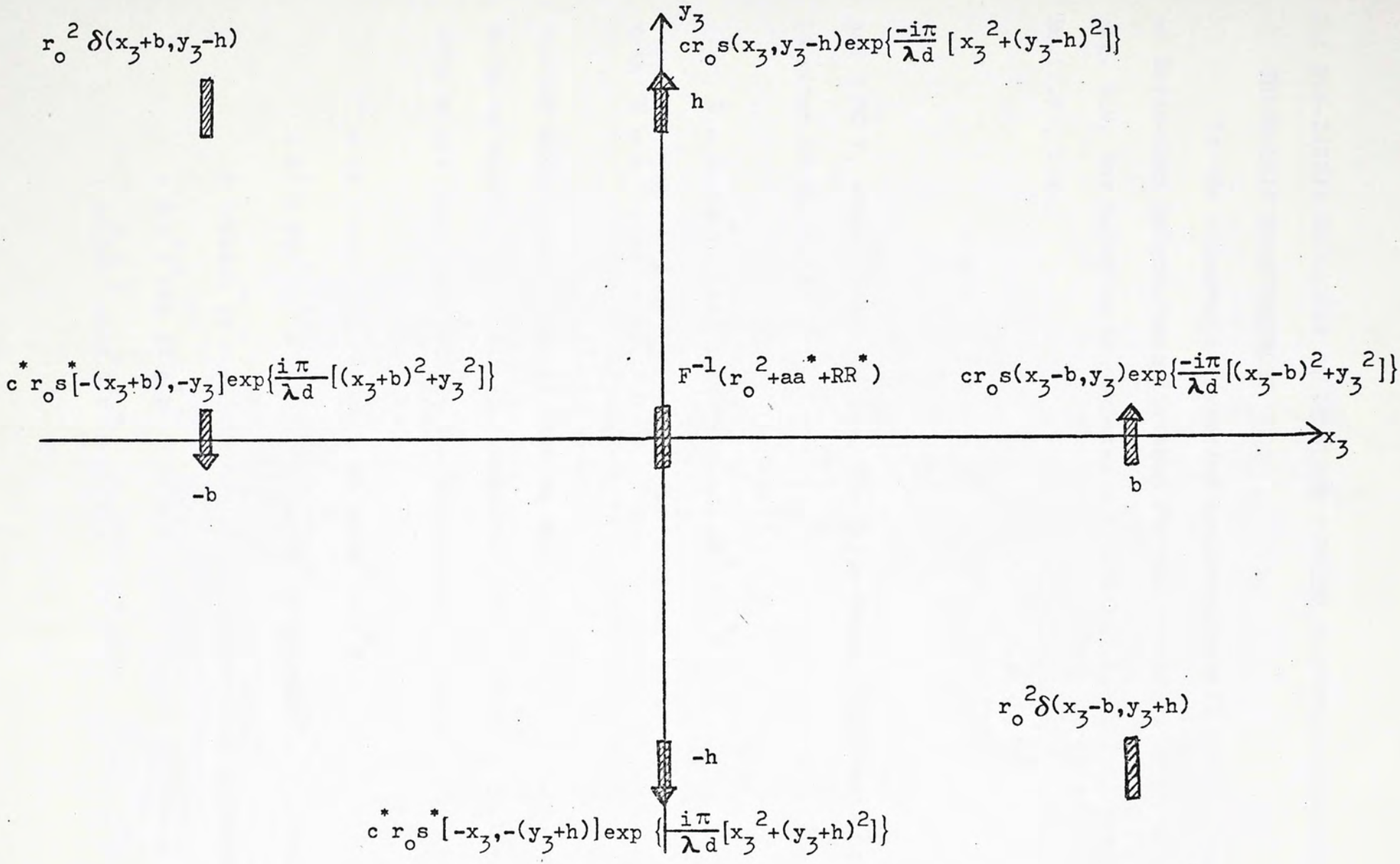

Fig. 2.7 Images reconstructed on the image plane with three-beam interference lensless Fourier transform hologram

2.6 NON-LINEAR RECORDING OF LENSLESS FOURIER TRANSFORM HOLOGRAM WITH THREE-BEAM INTERFERENCE

If the hologram is recorded nonlinearly with the arrangement of three-beam interference lensless Fourier transform as shown in Fig. 2.6, the hologram transmittance t after processing is given by Eq.(2.8), i.e.

$$t = c_o + c_1 E + c_2 E^2 + c_3 E^3 + \cdots\cdots$$

and $E \propto I$, where the intensity I of the three-beam interference pattern is given by Eq.(2.14),

$$I = K + a^* r + a r^* + a R^* + a^* R + r R^* + r^* R$$

with $K = r_o^2 + a a^* + R R^*$

The 1st order term $c_1 E$ gives rise to the reconstructed images same as shown in Section 2.5. And the quadratic terms producing nonlinear effects are terms included in the expression I^2, where

$$\begin{aligned} I^2 &= (K + a^* r + a r^* + a^* R + a R^* + r R^* + r^* R)^2 \\ &= K^2 + 2aa^* rr^* + 2RR^* rr^* + 2aa^* RR^* + (2K+2RR^*)a^* r + (2K+2RR^*)a r^* \\ &\quad + (2K+2aa^*)r^* R + (2K+2aa^*)r R^* + (2K+2rr^*)a^* R + (2K+2rr^*)a R^* \\ &\quad + 2(r^*)^2 aR + 2R^2 a^* r^* + 2r^2 a^* R^* + 2(R^*)^2 ar + 2a^2 r^* R^* + 2(a^*)^2 rR \\ &\quad + (r^*)^2 R^2 + (R^*)^2 r^2 + a^2 (r^*)^2 + (a^*)^2 r^2 + (a^*)^2 R^2 + a^2 (R^*)^2 \end{aligned}$$

$$= K_1 + [K_2 ar^* + K_2 a^* r + K_3 r^* R + K_3 r R^* + K_4 a^* R + K_4 a R^*]_1$$
$$+ [2(r^*)^2 aR + 2r^2 a^* R^* + 2R^2 a^* r^* + 2(R^*)^2 ar + (r^*)^2 R^2 + r^2 (R^*)^2]_2$$
$$+ [2a^2 r^* R^* + 2(a^*)^2 rR + a^2 (r^*)^2 + (a^*)^2 r^2 + (a^*)^2 R^2 + a^2 (R^*)^2]_3 \quad (2.17)$$

where $K_1 = K^2 + 2aa^* rr^* + 2RR^* rr^* + 2aa^* RR^*$

$K_2 = 2K + 2RR^*$

$K_3 = 2K + 2aa^*$

$K_4 = 2K + 2rr^*$

The brackets and subscripts are introduced for the convience of discussion. Plane wave illuminates the hologram as shown in Fig.2.3, with a lens placed before or after of the hologram to carry out the inverse Fourier transform of the hologram transmittance, $c_1 E + c_2 E^2$, which is proportional to a linear sum of Eq.(2.14) and Eq.(2.17) according to Eq.(2.8) .

In Eq. (2.17), the zero-order term K_1 is focused to the origin of the image plane. Locations of the first order images are given by inverse Fourier transforms of ar^*, $a^* r$, aR^*, $a^* R$, $r^* R$ and rR^* in $[\ ]_1$, as calculated in Eq. (2.5), Eq.(2.6), Eq.(2.11), Eq.(2.12), Eq.(2.15) and Eq.(2.16). These locations are the same as in Fig.2.7. The quadratic terms in $[\ ]_2$ giving rise to non-linear effects are inverse Fourier transformed to indicate locations of the higher order images.

$$\iint (r^*)^2 aR \exp[-2\pi i(\xi x_3 + \eta y_3)]\, d\xi\, d\eta$$
$$= c r_0^3 \iint S(\xi, \eta) \exp(4i\pi \xi b) \exp(-2i\pi \eta h) \exp[-2\pi i(\xi x_3 + \eta y_3)]\, d\xi\, d\eta$$

$$= cr_o^3 s(x_3-2b, y_3+h) \exp\left\{\frac{-i\pi}{\lambda d}\left[(x_3-2b)^2 + (y_3+h)^2\right]\right\} \qquad (2.18)$$

$$\iint r^2 a^* R^* \exp\left[-2\pi i(\xi x_3 + \eta y_3)\right] d\xi\, d\eta$$

$$= c^* r_o^3 \iint S^*(\xi,\eta)\exp(-4i\pi\xi b)\exp(2i\pi\eta h)\exp\left[-2\pi i(\xi x_3+\eta y_3)\right] d\xi d\eta$$

$$= c^* r_o^3 s^*\left[-(x_3+2b), -(y_3-h)\right] \exp\left\{\frac{i\pi}{\lambda d}\left[(x_3+2b)^2 + (y_3-h)^2\right]\right\} \qquad (2.19)$$

$$\iint R^{*2} ar \exp\left[-2\pi i(\xi x_3 + \eta y_3)\right] d\xi\, d\eta$$

$$= cr_o^3 \iint S(\xi,\eta)\exp(-2i\pi\xi b)\exp(4i\pi\eta h)\exp\left[-2\pi i(\xi x_3+\eta y_3)\right] d\xi d\eta$$

$$= cr_o^3 s(x_3+b, y_3-2h)\exp\left\{\frac{-i\pi}{\lambda d}\left[(x_3+b)^2 + (y_3-2h)^2\right]\right\} \qquad (2.20)$$

$$\iint R^2 a^* r^* \exp\left[-2\pi i(\xi x_3 + \eta y_3)\right] d\xi\, d\eta$$

$$= c^* r_o^3 \iint S^*(\xi,\eta)\exp(2i\pi\xi b)\exp(-4i\pi\eta h)\exp\left[-2\pi i(\xi x_3+\eta y_3)\right] d\xi d\eta$$

$$= c^* r_o^3 S^*\left[-(x_3-b), -(y_3+2h)\right] \exp\left\{\frac{i\pi}{\lambda d}\left[(x_3-b)^2 + (y_3+2h)^2\right]\right\} \qquad (2.21)$$

$$\iint (r^*)^2 R^2 \exp\left[-2\pi i(\xi x_3 + \eta y_3)\right] d\xi\, d\eta$$

$$= r_o^4 \iint \exp(4i\pi\xi b)\exp(-4i\pi\eta h)\exp\left[-2\pi i(\xi x_3+\eta y_3)\right] d\xi\, d\eta$$

$$= r_o^4\, \delta(x_3-2b,\ y_3+2h) \qquad (2.22)$$

$$\iint r^2 (R^*)^2 \exp\left[-2\pi i(\xi x_3 + \eta y_3)\right] d\xi\, d\eta$$

$$= r_o^4 \iint \exp(-4i\pi\xi b)\exp(4i\pi\eta h)\exp\left[-2\pi i(\xi x_3+\eta y_3)\right] d\xi\, d\eta$$

$$= r_o^4\, \delta(x_3+2b,\ y_3-2h) \qquad (2.23)$$

Inverse Fourier transform of other terms in $[\ ]_3$ consist of a^2 or $(a^*)^2$ is quite complicated so that only qualitative analysis is done.

$$a^2 r^* R^* = c^2 r_o^2 [S(\xi, \eta)]^2 \exp(2\pi i \xi b) \exp(2\pi i \eta h) \tag{2.24}$$

$$(a^*)^2 rR = (c^*)^2 r_o^2 [S^*(\xi, \eta)]^2 \exp(-2\pi i \xi b) \exp(-2\pi i \eta h) \tag{2.25}$$

$$a^2 (r^*)^2 = c^2 r_o^2 [S(\xi, \eta)]^2 \exp(4\pi i \xi b) \tag{2.26}$$

$$(a^*)^2 r^2 = (c^*)^2 r_o^2 [S^*(\xi, \eta)]^2 \exp(-4\pi i \xi b) \tag{2.27}$$

$$a^2 (R^*)^2 = c^2 r_o^2 [S(\xi, \eta)]^2 \exp(4\pi i \eta h) \tag{2.28}$$

$$(a^*)^2 R^2 = (c^*)^2 r_o^2 [S^*(\xi, \eta)]^2 \exp(-4\pi i \eta h) \tag{2.29}$$

The reconstructed images on the image plane are shown schematically in Fig. 2.8 .

As discussed in Section 2.4, inverse Fourier transformation of Eq. (2.24) to Eq.(2.29) contain the intermodulation terms and give higher order images coincide with the 1st order images other than those higher order images as located in Fig. 2.8. Similarly, we show only image locations of a subject point source in Fig.2.8 in order to simplify the figure.

Nonlinear effects produced by cubic terms are included in the expression I^3, where

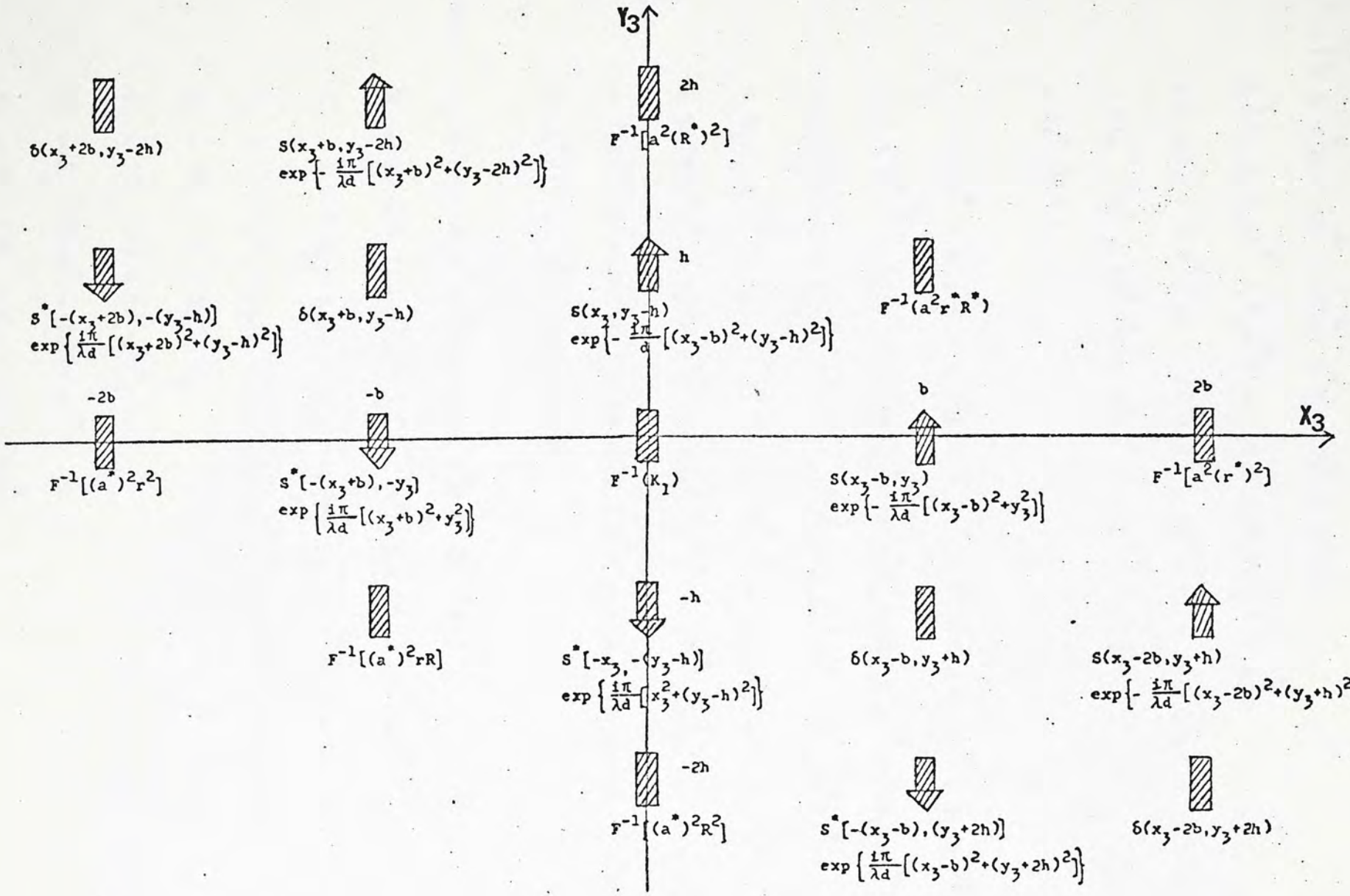

Fig. 2.8 Images reconstructed in the image plane with nonlinearly recorded three-beam interference Fourier transform hologram up to quadratic nonlinear effects

$$I^3 = [K + a^*r + ar^* + aR^* + a^*R + rR^* + r^*R]$$

$$x [K_1 + K_2 ar^* + K_2 a^* r + K_3 r^* R + K_3 rR^* + K_4 a^* R$$

$$+ K_4 aR^* + 2(r^*)^2 aR + 2r^2 a^* R^* + 2R^2 a^* r^* + 2(R^*)^2 ar + 2a^2 r^* R^*$$

$$+ 2(a^*)^2 rR + (r^*)^2 R^2 + r^2 (R^*)^2 + a^2 (r^*)^2 + (a^*)^2 r^2 + a^2 (R^*)^2$$

$$+ (a^*)^2 R^2]$$

$$= D_1 + D_2 ar^* + D_2 a^* r + D_3 r^* R + D_3 rR^* + D_4 a^* R + D_4 aR^* + D_5 (R^*)^2 ar$$

$$+ D_5 R^2 a^* r^* + D_6 (r^*)^2 aR + (D_6 - 1) r^2 a^* R^* + D_7 (R^* r)^2 + (D_7 - rr^*)(Rr^*)^2$$

$$+ D_8 (a^*)^2 rR + D_8 a^2 r^* R^* + D_9 (ar^*)^2 + D_9 (a^* r)^2 + D_{10} (a^* R)^2$$

$$+ D_{10} (aR^*)^2 + 3a(r^*)^3 R^2 + 3ar^2 (R^*)^3 + 3a^* (r^*)^2 R^3 + 3a^* r^3 (R^*)^2$$

$$+ 3a^2 R(r^*)^3 + 3a^2 r(R^*)^3 + 3(a^*)^2 r^3 R^* + 3(a^*)^2 r^* R^3 + 3a^3 r^* (R^*)^2$$

$$+ 3(a^*)^3 rR^2 + 2a^3 (r^*)^2 R^* + 2(a^*)^3 r^2 R + (ar^*)^3 + (a^* r)^3 + (aR^*)^3$$

$$+ (a^* R)^3 + (R^* r)^3 + (r^* R)^3 \qquad (2.30)$$

where $D_1 = KK_1 + 2K_2 a^* rr^* a + 2K_3 rR^* r^* R + 2K_4 a^* RaR^*$

$D_2 = K_1 + K_1 K_2 + a^* rr^* a + 2rR^* r^* R + K_4 RR^* + 2a^* RaR^* + K_3 RR^*$

$D_3 = K_1 + K_1 K_3 + K_2 aa^* + K_4 aa^* + 2rr^* aa^* + r^* RR^* r + 2a^* aRR^*$

$D_4 = K_1 + K_1 K_4 + K_2 rr^* + K_3 rr^* + 2ar^* a^* r + 2R^* rr^* R + aR^* a^* R$

$D_5 = 2K_1 + 2 + K_3 + K_4$

$D_6 = 2K_1 + 2 + K_2 + K_3$

$D_7 = K_1 + 4aa^* + K_3 + rr^*$

$D_8 = 2K_1 + K_2 + K_4 + rr^* + RR^*$

$$D_9 = K_1 + K_2 + 4RR^*$$

$$D_{10} = K_1 + K_4 + 4rr^*$$

Images reconstructed by the nonlinearly recorded hologram up to cubic nonlinear effects with plane wave illumination are inverse Fourier transform of the hologram transmittance proportional to sum of Eq.(2.14), Eq.(2.17) and Eq.(2.30). In addition to images given by Eq.(2.5), Eq.(2.6), Eq.(2.11), Eq.(2.12) , Eq.(2.15), Eq.(2.16) and Eq.(2.18) to Eq.(2.23), there are more images given by the inverse Fourier transform as following,

$$\iint a(r^*)^3 R^2 \exp\left[-2\pi i(\xi x_3+\eta y_3)\right] d\xi\, d\eta$$

$$= c r_o^5 \iint S(\xi,\eta)\exp(6\pi i\xi b)\exp(-4\pi i\eta h)\exp\left[-2\pi i(\xi x_3+\eta y_3)\right] d\xi\, d\eta$$

$$= c r_o^5 s(x_3-3b, y_3+2h)\exp\left\{\frac{-i\pi}{\lambda d}\left[(x_3-3b)^2+(y_3-2h)^2\right]\right\}$$

$$\iint a r^2 (R^*)^3 \exp\left[-2\pi i(\xi x_3+\eta y_3)\right] d\xi\, d\eta$$

$$= c r_o^5 \iint S(\xi,\eta)\exp(-4\pi i\xi b)\exp(6\pi i\xi b)\exp\left[-2\pi i(\xi x_3+\eta y_3)\right] d\xi\, d\eta$$

$$= c r_o^5 s(x_3+2b, y_3-3h)\exp\left\{\frac{-i\pi}{\lambda d}\left[(x_3+2b)^2+(y_3-3h)^2\right]\right\}$$

$$\iint a^*(r^*)^2 R^3 \exp\left[-2\pi i(\xi x_3+\eta y_3)\right] d\xi\, d\eta$$

$$= c^* r_o^5 \iint S^*(\xi,\eta)\exp(4\pi i\xi b)\exp(-6\pi i\eta h)\exp\left[-2\pi i(\xi x_3+\eta y_3)\right] d\xi\, d\eta$$

$$= c^* r_o^5 S^*\left[-(x_3-2b), -(y_3+3h)\right]\exp\left\{\frac{i\pi}{\lambda d}\left[(x_3-2b)^2+(y_3+3h)^2\right]\right\}$$

$$\iint a^* r^3 (R^*)^2 \exp\left[-2\pi i(\xi x_3 + \eta y_3)\right] d\xi\, d\eta$$

$$= c^* r_o^5 \iint S^*(\xi,\eta)\exp(-6\pi i \xi b)\exp(4\pi i \eta h)\exp\left[-2\pi i(\xi x_3 + \eta y_3)\right] d\xi\, d\eta$$

$$= c^* r_o^5 S^*\left[-(x_3+3b), -(y_3-2h)\right]\exp\left\{\frac{i\pi}{\lambda d}\left[(x_3+3b)^2 + (y_3-2h)^2\right]\right\}$$

$$\iint (R^* r)^3 \exp\left[-2\pi i(\xi x_3 + \eta y_3)\right] d\xi\, d\eta$$

$$= r_o^6 \iint \exp(-6\pi i \xi b)\exp(6\pi i \eta h)\exp\left[-2\pi i(\xi x_3 + \eta y_3)\right] d\xi\, d\eta$$

$$= r_o^6\, \delta(x_3+3b,\ y_3-3h)$$

$$\iint (R r^*)^3 \exp\left[-2\pi i(\xi x_3 + \eta y_3)\right] d\xi\, d\eta$$

$$= r_o^6 \iint \exp(6\pi i \xi b)\exp(-6\pi i \eta h)\exp\left[-2\pi i(\xi x_3 + \eta y_3)\right] d\xi\, d\eta$$

$$= r_o^6\, \delta(x_3-3b,\ y_3+3h)$$

Terms involve a^2, $(a^*)^2$, a^3, $(a^*)^3$ cannot give the original subject image but produce a set of flare lights to disturb the reconstructed images. In addition to those with locations indicated by Eq.(2.24) to Eq.(2.29), more terms are analyzed in the following,

$$a^2 R (r^*)^3 = c^2 r_o^4 \left[S(\xi,\eta)\right]^2 \exp(6\pi i \xi b)\exp(-2\pi i \eta h)$$

$$a^2 r (R^*)^3 = c^2 r_o^4 \left[S(\xi,\eta)\right]^2 \exp(-2\pi i \xi b)\exp(6\pi i \eta h)$$

$$(a^*)^2 r^* R^3 = (c^*)^2 r_o^4 \left[S^*(\xi,\eta)\right]^2 \exp(2\pi i \xi b)\exp(-6\pi i \eta h)$$

$$a^3 r^* (R^*)^2 = c^3 r_o^3 \left[S(\xi,\eta)\right]^3 \exp(2\pi i \xi b)\exp(4\pi i \eta h)$$

$$(a^*)^2 r^3 R^* = (c^*)^2 r_o^4 \left[S^*(\xi, \eta) \right]^2 \exp(-6\pi i \xi b) \exp(2\pi i \eta h)$$

$$a^3 (r^*)^2 R^* = c^3 r_o^3 \left[S(\xi, \eta) \right]^3 \exp(4\pi i \xi b) \exp(2\pi i \eta h)$$

$$(a^*)^3 r^2 R = (c^*)^3 r_o^3 \left[S^*(\xi, \eta) \right]^3 \exp(-4\pi i \xi b) \exp(-2\pi i \eta h)$$

$$(a^*)^3 r R^2 = (c^*)^3 r_o^3 \left[S^*(\xi, \eta) \right]^3 \exp(-2\pi i \xi b) \exp(-4\pi i \eta h)$$

$$(a r^*)^3 = c^3 r_o^3 \left[S(\xi, \eta) \right]^3 \exp(6\pi i \xi b)$$

$$(a^* r)^3 = (c^*)^3 r_o^3 \left[S^*(\xi, \eta) \right]^3 \exp(-6\pi i \xi b)$$

$$(a R^*)^3 = c^3 r_o^3 \left[S(\xi, \eta) \right]^3 \exp(6\pi i \eta h)$$

$$(a^* R)^3 = (c^*)^3 r_o^3 \left[S^*(\xi, \eta) \right]^3 \exp(-\pi i \eta h)$$

Inverse Fourier transformation of the above terms also give higher order images coincide with the 1st and 2nd order images. These higher order images due to intermodulation terms are in fact false images of point sources that are not actually present on the subject.

The reconstructed images on the image plane are shown schematically in Fig.2.9 with the assumption of point subject.

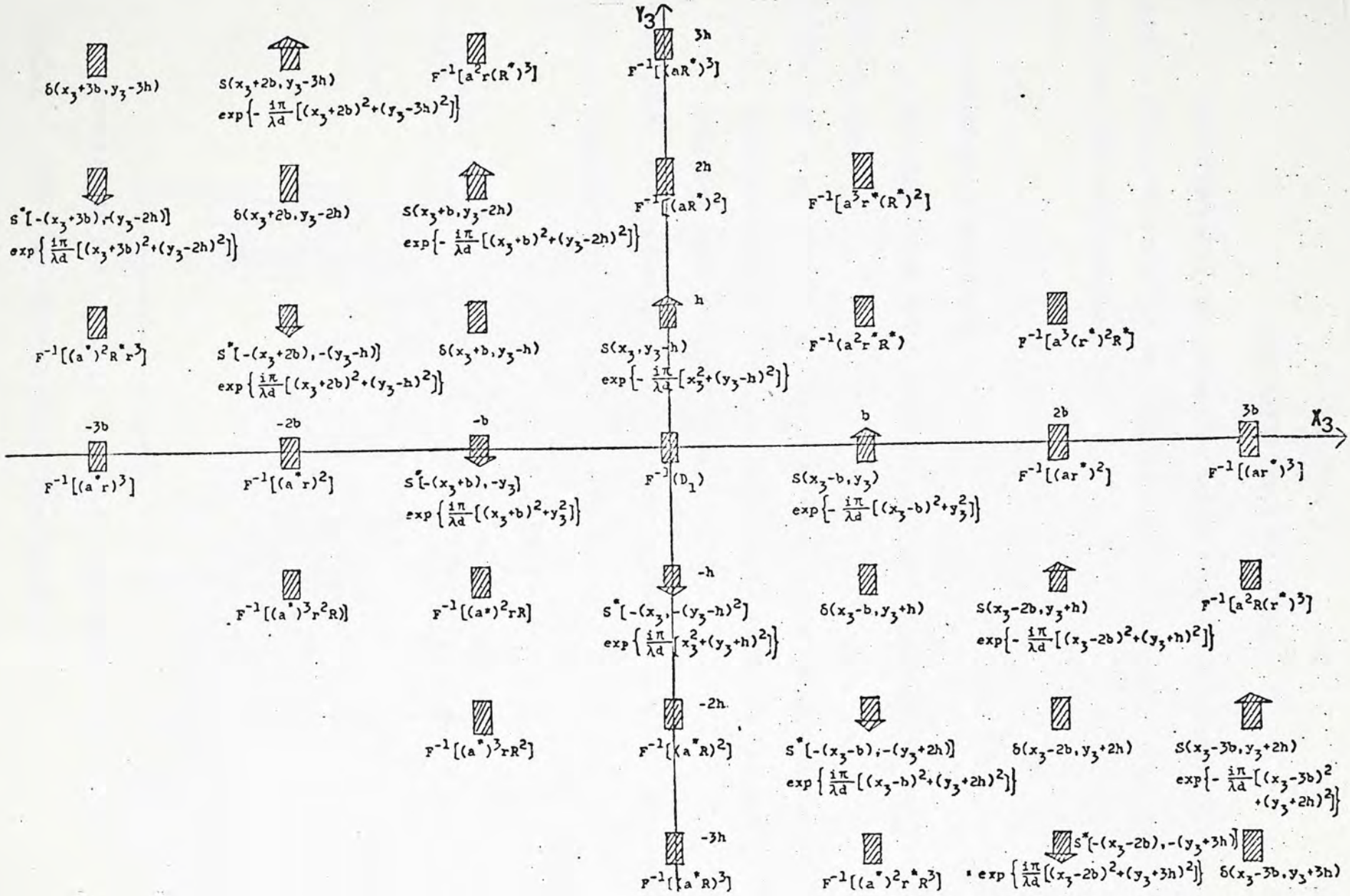

Fig. 2.9 Images reconstructed in the image plane with nonlinearly recorded three-beam interference Fourier transform holograms up to cubic nonlinear effects

CHAPTER 3

EXPERIMENTAL TECHNIQUES

The apparatus and experimental set up in this work is very simple. The processes can be divided into three steps which are described in this chapter.

3.1 RECORDING OF HOLOGRAMS

The apparatus and necessary optical components in the recording process are :

He-Ne laser —— The Spectra Physics Model 120 cw Helium-Neon Gas laser provides greater than 5 milliwatts of power at 632.8nm (visible red) at TEM_{oo} mode.

Michaelson Interferometer —— Top view of the Beck-Ealing Michaelson Interferometer is shown in Fig. 3.1 .

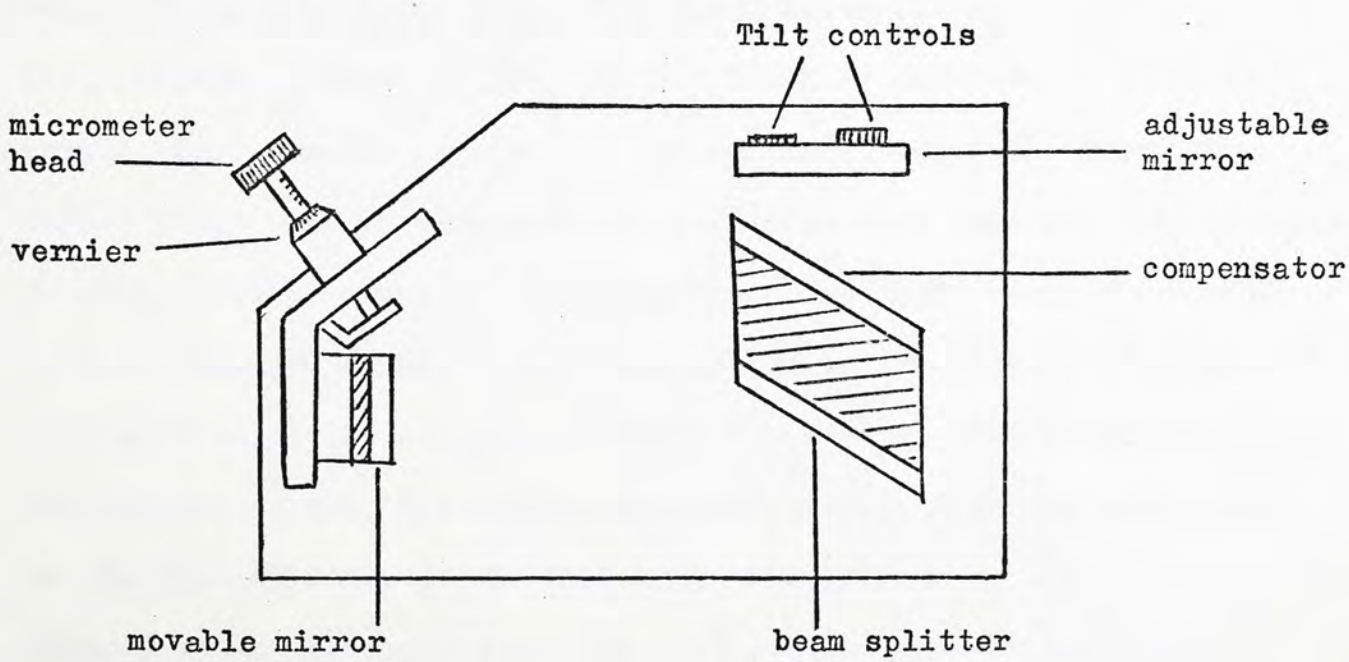

Fig.3.1 Top view of Michaelson Interferometer

double concave lens	diameter = 9.5 mm
	focal length = -4.5 mm
double convex lens	diameter = 3.9 cm
	focal length = 50 mm
plano-convex lens	diameter = 2.1 cm
	focal length = 50 mm

The light source used in recording is the 6328A red line from a He-Ne laser. A Michaelson Interferometer is used as the beam splitter. The advantage of using a Michaelson Interferometer as a beam splitter is that small interbeam angle can be obtained with suitable adjustment of the tilt controls. The experimental set up is shown schematically in Fig. 3.2 .

To ensure a steady fringe pattern, all optical components as well as the subject, the light source, the Michaelson Interferometer, and the recording medium are carefully set up on a concrete table supported by four motor cycle tire inner tubes filled with air at a low pressure to absorb vibration. The laser is adjusted so that the output light beam is parallel to the surface of optical table. The output laser beam is expanded by a double concave lens and then passes through a double convex lens to collimate the light beam. The double concave lens and double convex lens should be laterally and vertically displaced until the collimated light beam has its centre coincide with the subject centre. The collimated laser beam is directed to incident on the beam splitter of the Michaelson Interferometer and amplitude divided by the beam splitter. One part of the laser beam then falls on the plane mirror M_1 and the other part falls on the mirror M_2 .

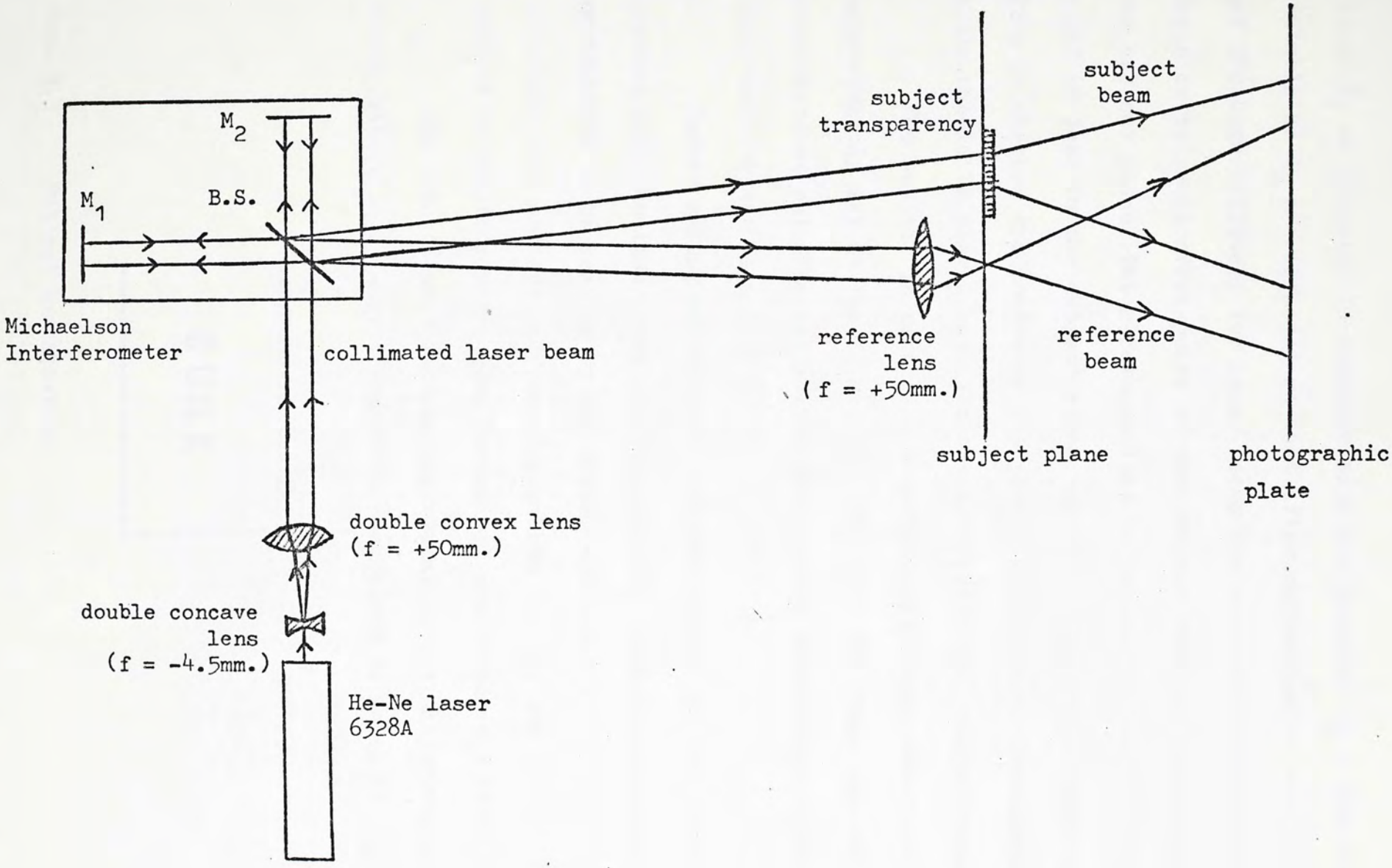

Fig. 3.2 Experimental set up for recording

First, M_1 is adjusted to coincide with the image of M_2 . Then the tilt controls of M_2 are adjusted so that after reflection at the two mirrors and the beam splitter, two laser beams are separated by a certain distance to avoid overlappimg of the subject beam and reference beam on the subject plane. The reference lens is located so that its focal point is just in the subject plane and the centre of the diverging beam from it strikes the centre of the photographic plate. The photographic plate should be placed with its normal towards the subject transparency.

The subject to reference beam intensity ratio should be approximately 1:1 at the film plane. However, the image can still be reconstructed satisfactorily with the subject to reference beam intensity ratio not greater than 10:1 .

Before making an exposure, let the system sit for about ten minutes with the laser running. This permits thermal and mechanical equilibrium to be reached by the system components. It is extremely important that all optical components used for the set up is not subject to building vibration, mechanical and airborne disturbances.

The subject used in this experiment is a transparency wi th black letters on a large transparent background as shown in Fig. 3.3.

Fig. 3.3 Subject transparency

A magic transparent tape (Scotch Brand) is stuck on the subject transparency and acted as a diffuser.

In recording a two-beam lensless Fourier transform hologram, the diffused subject wave interferes with the spherical reference wave on the photographic plate to form a two-beam interference pattern. If a three-beam interference lensless Fourier transform hologram is recorded, the additional reference beam is introduced by making a small hole underneath the subject letters as shown in Fig. 3.4 .

Fig. 3.4 Subject transparency with a small hole as the second reference source.

The hole is made as close to the subject letters as possible, and it is made sufficiently small, so that it can be treated as a second reference point source. However, it is practically impossible to make the hole as small as the focal point of the laser beam by a double convex lens. If the illuminating beam is divided into two parts, so that one part of it illuminates the subject transparency and the other part is focused to a point in the subject plane, then it is impossible to place the second reference source as close to the subject

letters as a hole is made.

In this experiment, the second reference source is not really a point but a circle of diameter about 5 mm. However, this diameter is still small compare to the size of the subject and distance of the subject plane to the hologram plane, thus it can still be treated as a point and light passes through this point plays the role of the second reference source.

A double convex lens is placed before the subject transparency to obtain diverge illuminating beam large enough to cover the subject letters, and the subject size is still small enough to assume constant amplitude illumination. The change of Fig. 3.2 for recording of three-beam interference hologram is shown in Fig. 3.5 .

As the subject lens is focused in a plane slightly behind the subject plane, the second reference source is not really a point source in the subject plane but in the focal plane of the subject lens. The hologram made by recording of the interference pattern of the diffused subject wave and the second spherical reference wave is the lensless Fourier transform hologram with a phase shift term. This phase shift cause the two reconstructed Fourier transform images to be in two slightly different image planes as expected [17].

Whether the holograms are recorded linearly or nonlinearly are controlled by their different exposure time. Nonlinearly recorded holograms usually have longer exposure time than those recorded linearly.

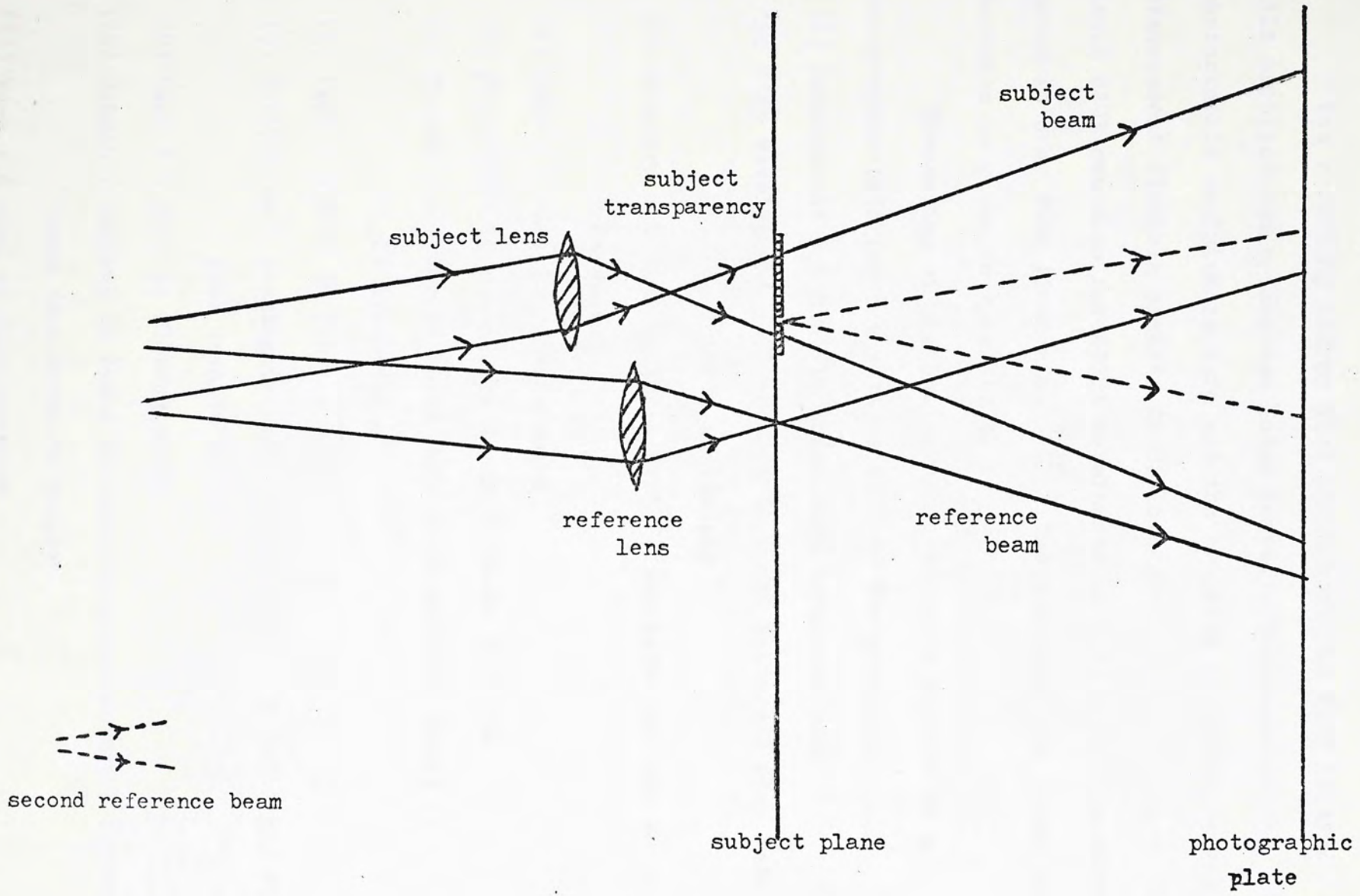

Fig. 3.5 Recording of three-beam interference lensless Fourier transform hologram

3.2 FILM PROCESSING [19]

The recording medium used throughout the work is type 649F film manufactured by Eastman Kodak company. Thickness of the photographic emulsion is 6μm and the emulsion is coated over a transparent flexible acetate film. Intensity transmittance of the Kodak 649F emulsion for 6328A wavelength is 0.81 , and its resolving power is over 2000 lines/min. [18] The t-E curve for Kodak 649F emulsion is shown in Appendix V.

Processing of the photographic emulsion exposed to a holographic interference pattern follows the procedure :

(1) Development : 5 min. in Kodak D-19 developer bath

(2) Stop development : 30 seconds in Kodak Universal Stop Bath (with indicator)

(3) Fixation : 5 min. in Kodak Rapid Fixer bath (contain an emulsion hardener)

(4) Wash : 5 min. in flowing water

(5) Photo-Fo : 10 seconds in Kodak Photo-Fo solution

(6) Bleach : soaking in Kodak Mercury Intensifier until film is light blue-pink

(7) Wash : 5 min. in flowing water

(8) Refixation : soaking in Kodak Rapid Fixer bath until all blue-pink turn to brown

(9) Wash : 5 min. in flowing water

(10) Bleach : saoking in Kodak Chromium Intensifier until the film turns from brown to yellow

(11) Wash : 5 min. in flowing water

(12) Drying

In step (6), $HgCl_2$ is contained in the mercury intensifier and the chemical reaction is given by

$$\underset{\text{activated black}}{Hg} + HgCl_2 \longrightarrow \underset{\text{bluish-purple}}{AgHgCl_2}\downarrow$$

In step (8), $Na_2S_2O_3$ contained in the fixer is a reducing agent, which reduces $AgHgCl_2$ to Ag again. In step (10), the chemical reaction is given by

$$9Ag + 12NaCl + 7H_2SO_4 + (NH_4)_2Cr_2O_7 \longrightarrow$$

$$\underset{\text{colorless}}{9AgCl}\downarrow + \underset{\text{brown}}{Cr_2Cl_3}\downarrow + 7H_2O + 6Na_2SO_4 + (NH_4)_2SO_4$$

It is the AgCl colorless deposit which carries the information in the hologram. However, step (6) to step (8) may be skipped and go to step (10) directly. Experiments have been done and the results show that the holograms undergo only step (8) or step (10) do not have a high quality as that with two bleaching process [20].

Chemical contents of all the chemical processing aids used in the above procedure are recorded in detail in the book published by Eastman Kodak company [21], and the procedure is also recommended by this Company [22].

3.3 RECONSTRUCTION OF IMAGES

After necessary processing, the hologram is reconstructed with either white light source or He-Ne laser beam. The illuminating beam may be collimated so that plane wave of constant amplitude is incident on the hologram and the images are reconstructed with a convex lens. However, it is much simpler if diverging light or converging light is used in each case of different illuminating source.

The necessary optical components and apparatus used in reconstruction are :

He-Ne laser	The Spectra Physics Model 155 CW Helium-Neon Gas laser provides 0.5 milliwatts of power at 632.8 nm at TEM_{oo} mode
double concave lens	diameter = 9.5 mm focal length = -4.5 mm
double convex lens	(1) diameter = 4.5 cm focal length = +90 mm (2) diameter = 7 cm focal length = +300 mm
Mercury lamp	Beck 125 watt high pressure Mercury Vapour Lamp
Projector	Leitz 500 watt high power projector
diaphragms	(1) smallest diameter = 2 mm (2) smallest diameter = 1 mm

The photographic plate used for recording of reconstructed images is Kodak Panatomic-X Film or Kodacolor II color negative film.

If high pressure mercury vapour lamp or a high power projector is used as white light source in reconstruction, the experimental set

up for reconstruction is shown in Fig. 3.6 .

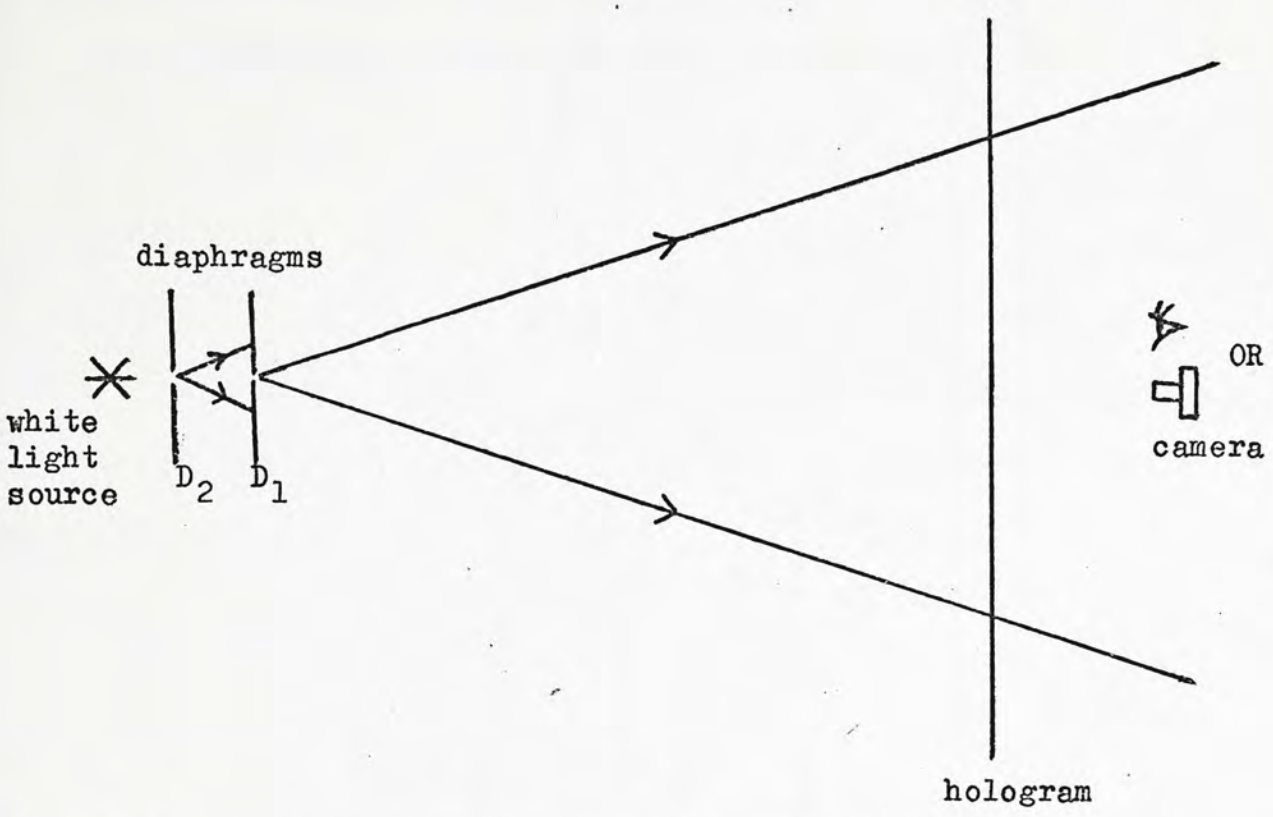

Fig. 3.6 Reconstruction with white light source

A diaphragm is placed before the extended white light source to obtain point illuminating source. Virtual images are reconstructed if the hologram is illuminated by the diverging illuminating light wave.

Experimental result has shown that if the size of the illuminating source is smaller, brighter images of higher resolution will be reconstructed. Thus two diaphragms are used in this work in reconstruction with white light source. Diaphragm D_1 of smallest diameter 1 mm is placed behind D_2 of smallest diameter 2 mm, so that the illuminating source is more resemble to an ideal point source. However, intensity of the illuminating wave will be much reduced in this way, and longer exposure time is needed in recording of the reconstructed virtual images with a camera. The viewer looks through

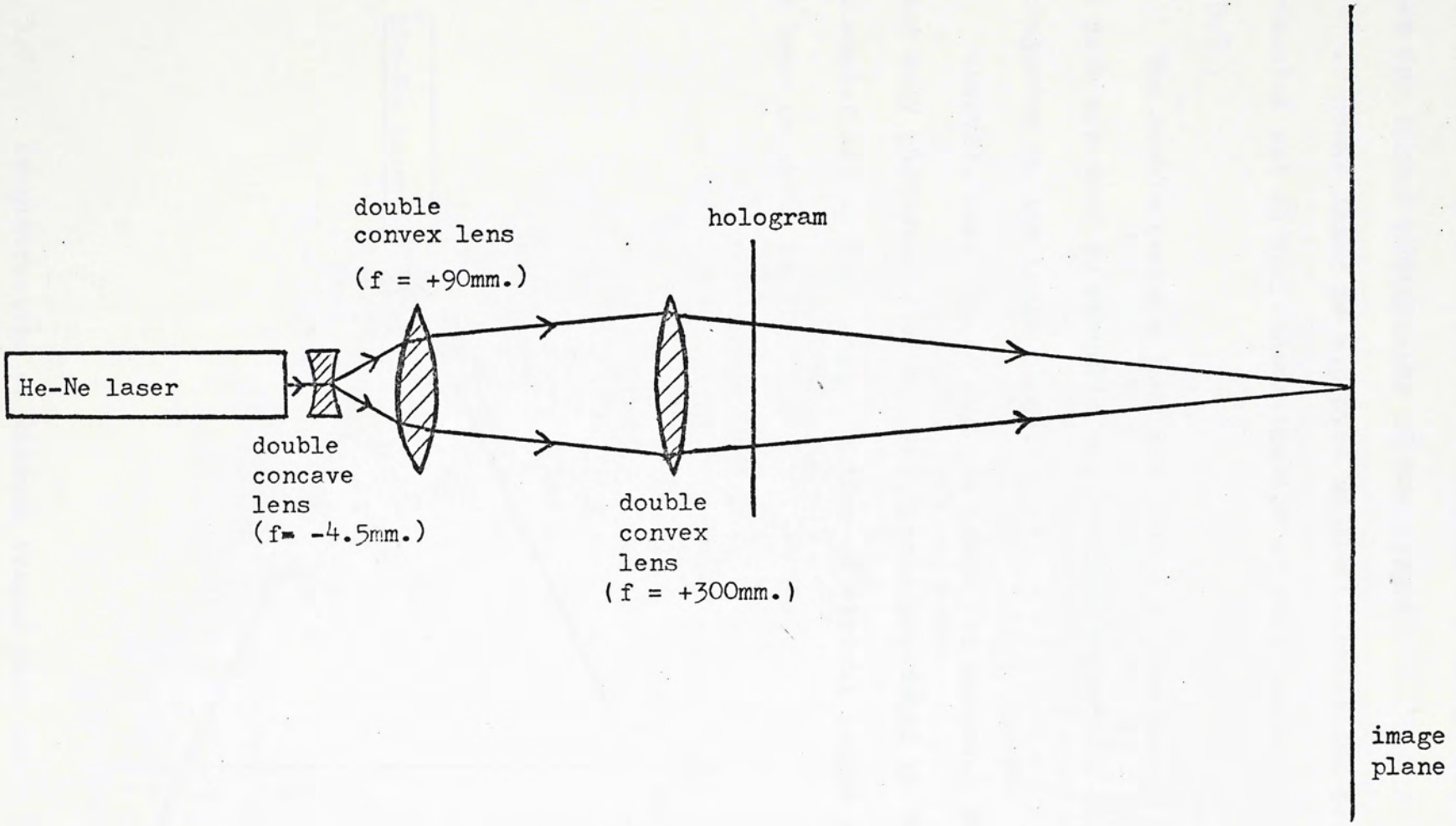

Fig. 3.7 Reconstruction of real images with He-Ne laser beam

the hologram can observe the virtual images clearly, and a camera can be used for taking photographs of the images.

If He-Ne laser is employed as the illuminating source, the experimental set up for reconstruction of real images is shown in Fig. 3.7 .

The double concave lens and double convex lenses placed in the light path are used to resemble the original reference beam. Real images are projected on the image plane.

However, real images are too large for entering the camera lens, so that only photographs of virtual images are taken in this work. Experimental set up for reconstruction of virtual images with He-Ne laser beam is shown in Fig. 3.8 .

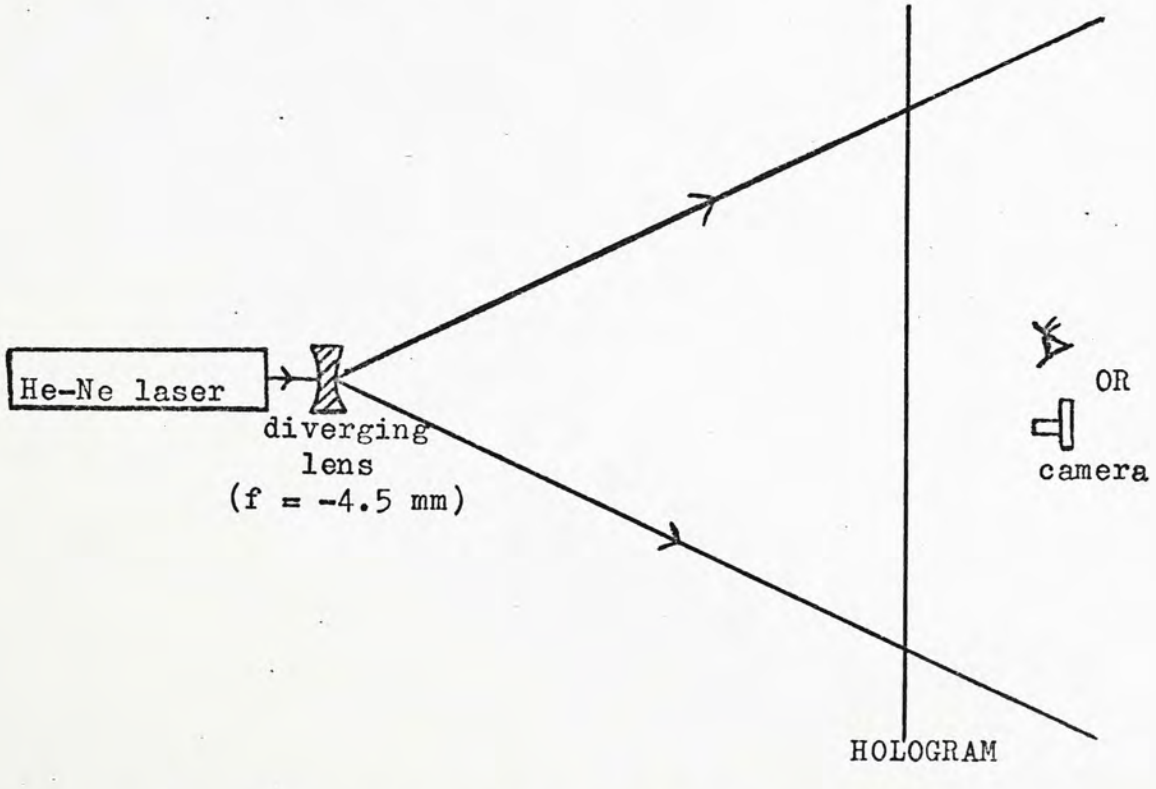

Fig. 3.8 Reconstruction of virtual images with He-Ne laser beam

A diverging lens is placed before the laser to expand the output laser beam and obtains the diverging illuminating beam. Also a camera can be placed close to the hologram and photographs of virtual images are taken with the virtual images focused on the film plane.

CHAPTER 4

RESULT AND DISCUSSION

4.1 ACHROMATIC IMAGES RECONSTRUCTED WITH INCOHERENT LIGHT WITH TWO-BEAM INTERFERENCE LENSLESS FOURIER TRANSFORM HOLOGRAM

The hologram for reconstruction of achromatic images is the recording of the holographic interference pattern of the diffused subject wave and the second reference wave. Since the second reference source is made as close to the subject as possible [see Section 3.1], the Fourier transform images can be reconstructed even with white light source (a Mercury Vapour Lamp or a high power projector as white light source) and with less color dispersion as discussed in Section 2.3.

Photographs of the achromatic Fourier transform images reconstructed with Hg lamp are shown in Fig. 4.1 and Fig. 4.2 . These two photographs are focused on the upper and the lower side images respectively. This confirms the prediction that two images will be focused on different focal plane as explained in Section 3.1 .

A photograph of the images reconstructed with He-Ne laser beam as shown in Fig. 4.3 shows no difference between images reconstructed with coherent light and incoherent light.

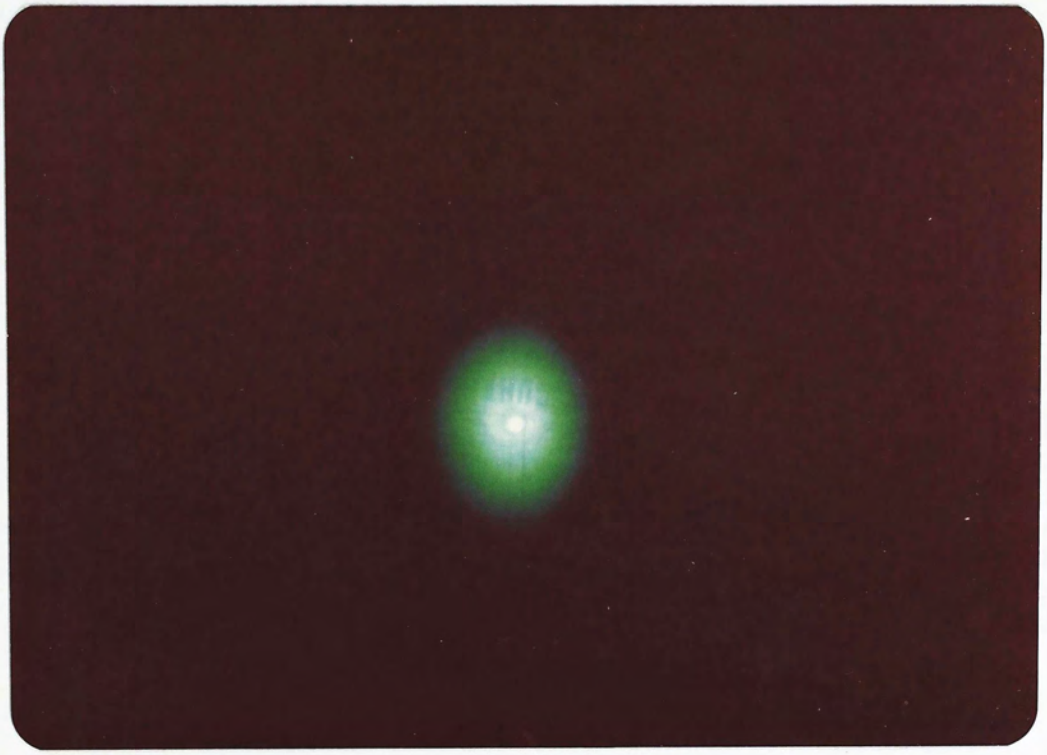

Fig.4.1 Achromatic image reconstructed with Hg lamp and focused on upper image

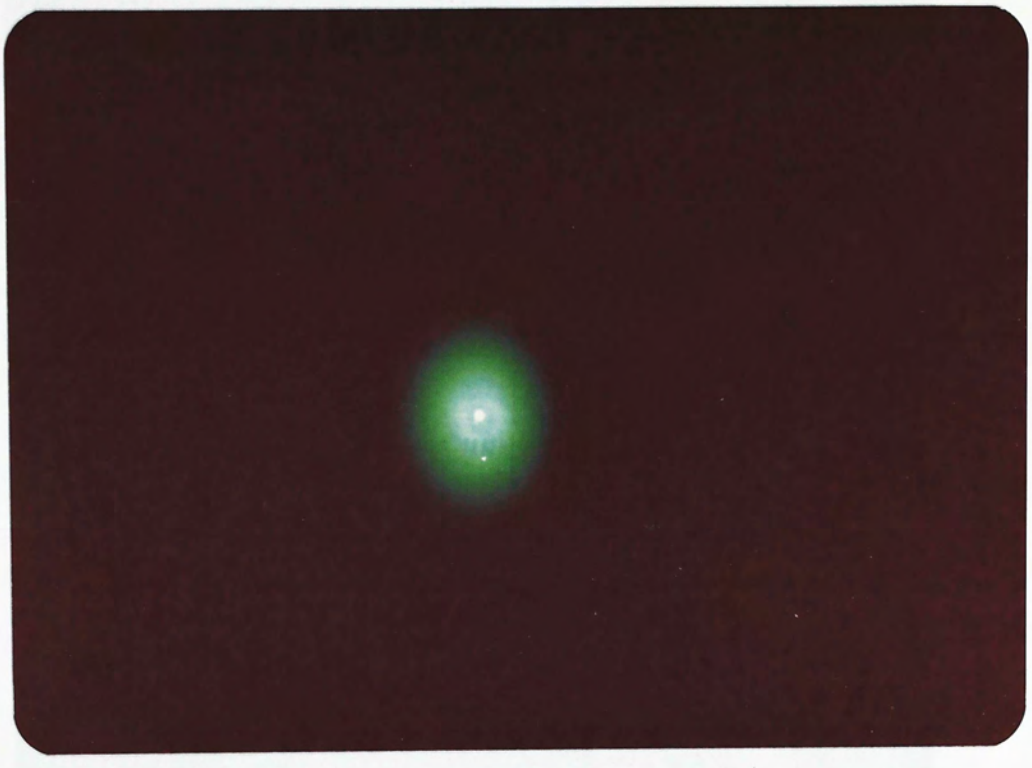

Fig.4.2 Achromatic image reconstructed with Hg lamp and focused on lower image

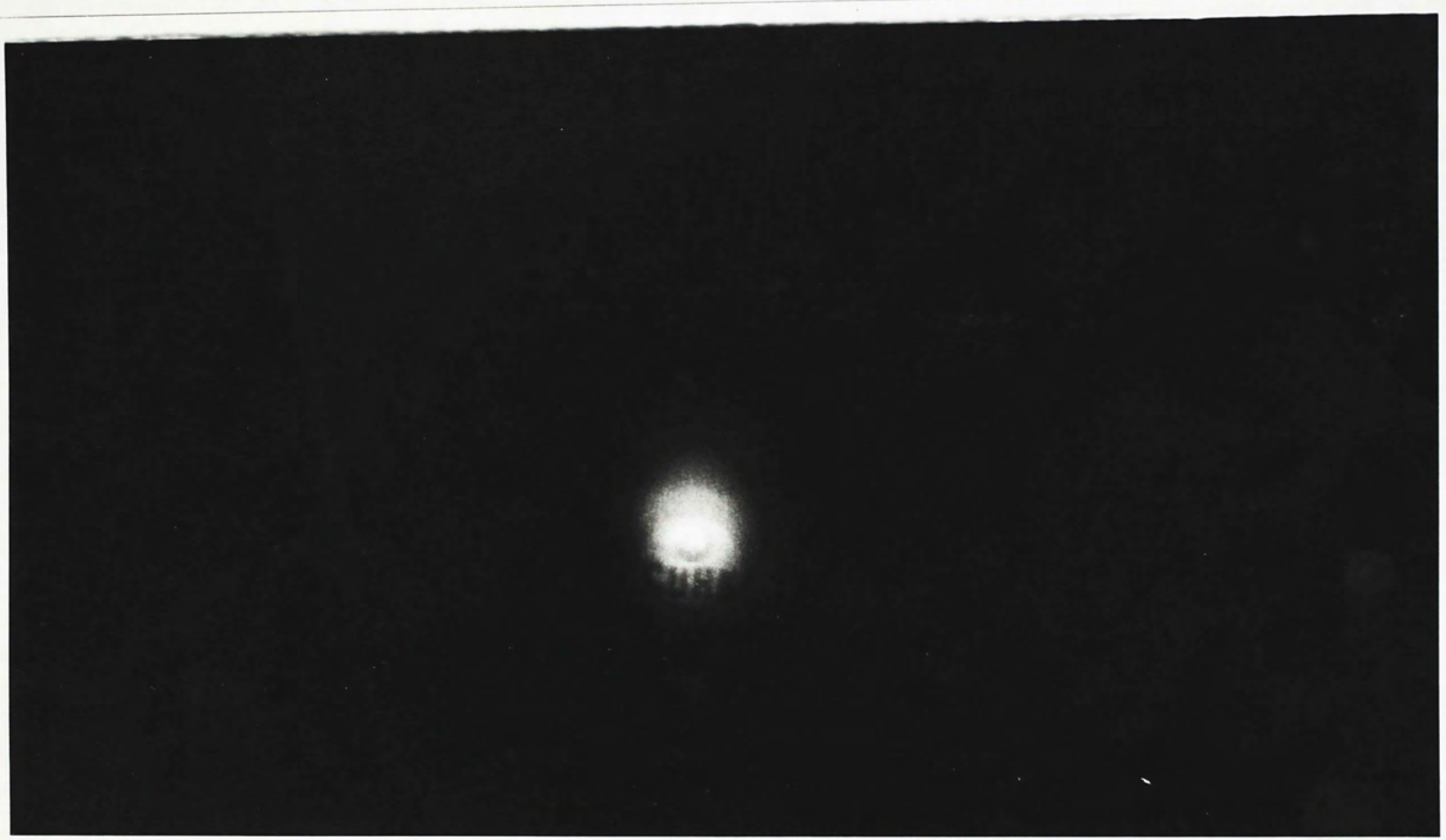

Fig.4.3 Images reconstructed with He-Ne laser

4.2 ACHROMATIC IMAGES RECONSTRUCTED WITH INCOHERENT LIGHT WITH NON-LINEARLY RECORDED THREE-BEAM INTERFERENCE LENSLESS FOURIER TRANSFORM HOLOGRAM

The hologram is recorded nonlinearly with the interference pattern of the diffused subject wave and two spherical reference waves. In reconstruction with Hg source and with the optical set up as shown in Fig. 3.6 , only 1st order images at the location of central zero-order are reconstructed, the other diffraction orders give only color dispersions with no clear subject letters. Photographs of the reconstructed achromatic images are shown in Fig. 4.4 and Fig. 4.5 , each focused on different images.

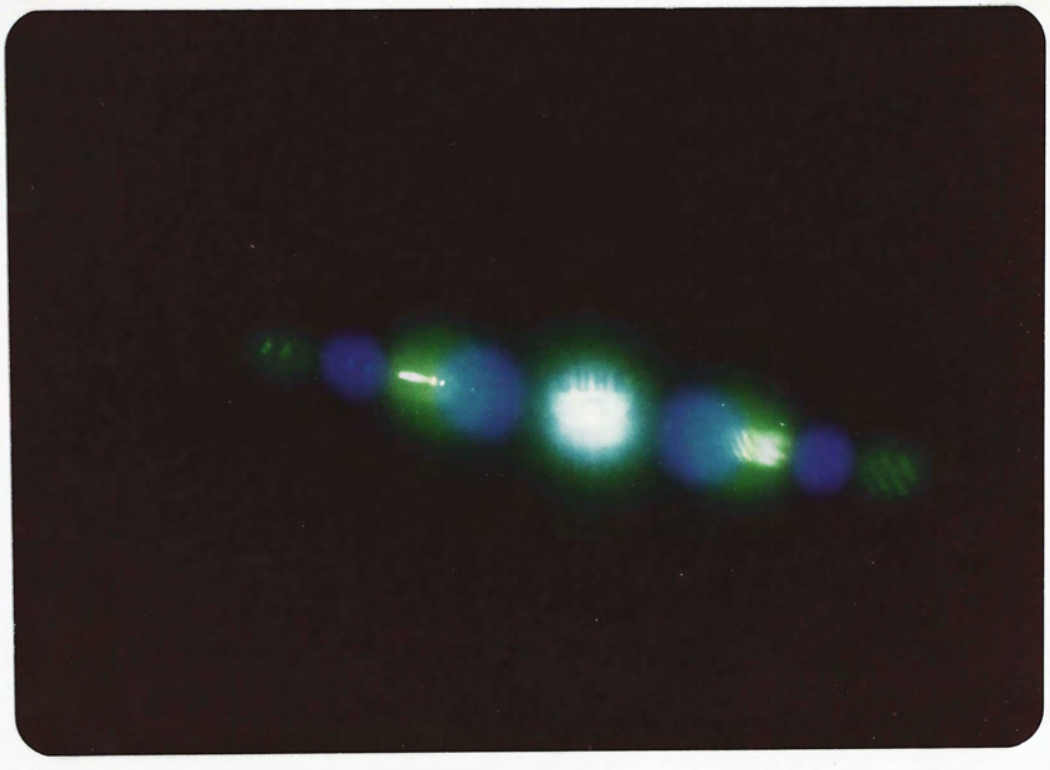

Fig. 4.4 Achromatic image reconstructed with Hg lamp with three-beam interference lensless Fourier transform hologram and focused on upper image

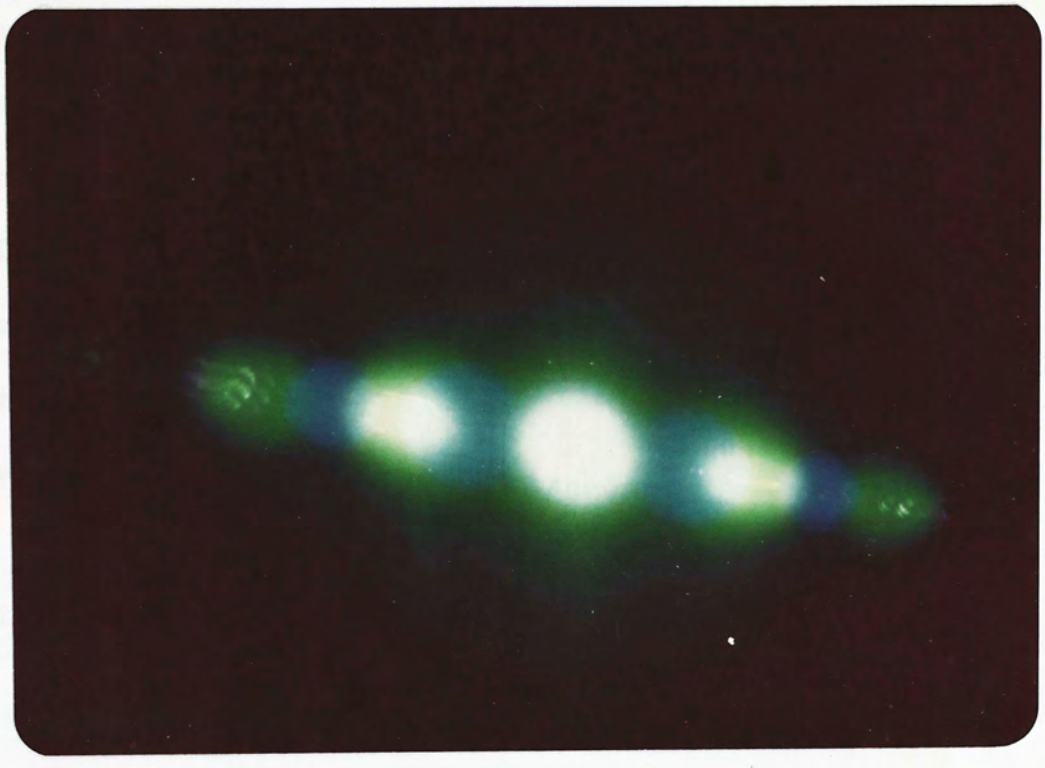

Fig.4.5 Achromatic image reconstructed with Hg lamp with three-beam interference lensless Fourier transform hologram and focused on lower image

4.3 RECONSTRUCTION OF IMAGE FROM NON-LINEAR RECORDED TWO-BEAM INTERFERENCE LENSLESS FOURIER TRANSFORM HOLOGRAM WITH He-Ne LASER

The hologram records nonlinearly the interference pattern of the diffused subject wave and the first spherical reference wave. In reconstruction with He-Ne laser beam, both first and second order images are reconstructed simultaneously. A photograph of the reconstructed images is shown in Fig. 4.6 .

It is noticed that only the subject letters in first diffraction order can be observed, while the letters in second diffraction order is blurred and cannot be read out. This is explained by the fact that only the subject wave a is reconstructed in 1st diffraction order of the hologram diffraction grating, and a^2 is reconstructed in 2nd order as derived in Section 2.4 .

Fig. 4.6 Images reconstructed with nonlinearly recorded two-beam interference lensless Fourier transform hologram

4.4 RECONSTRUCTION OF IMAGES FROM LINEARLY RECORDED THREE-BEAM INTERFERENCE LENSLESS FOURIER TRANSFORM HOLOGRAM WITH He-Ne LASER

The hologram is also a recording of the interference pattern of the diffused subject wave and two spherical reference waves as that in Section 4.2 . However, the hologram is now recorded linearly and reconstructed with He-Ne laser source. The optical arrangement for reconstruction is shown in Fig. 3.8 . A photograph of the reconstructed images is shown in Fig. 4.7 .

Images of 1st and higher diffraction orders are observable while images at the location of central zero-order still not appears. It is also noticed that the subject letters can be read out even in the 2nd diffraction order. This is the most important difference between a two-beam interference and three-beam interference Fourier transform holograms.

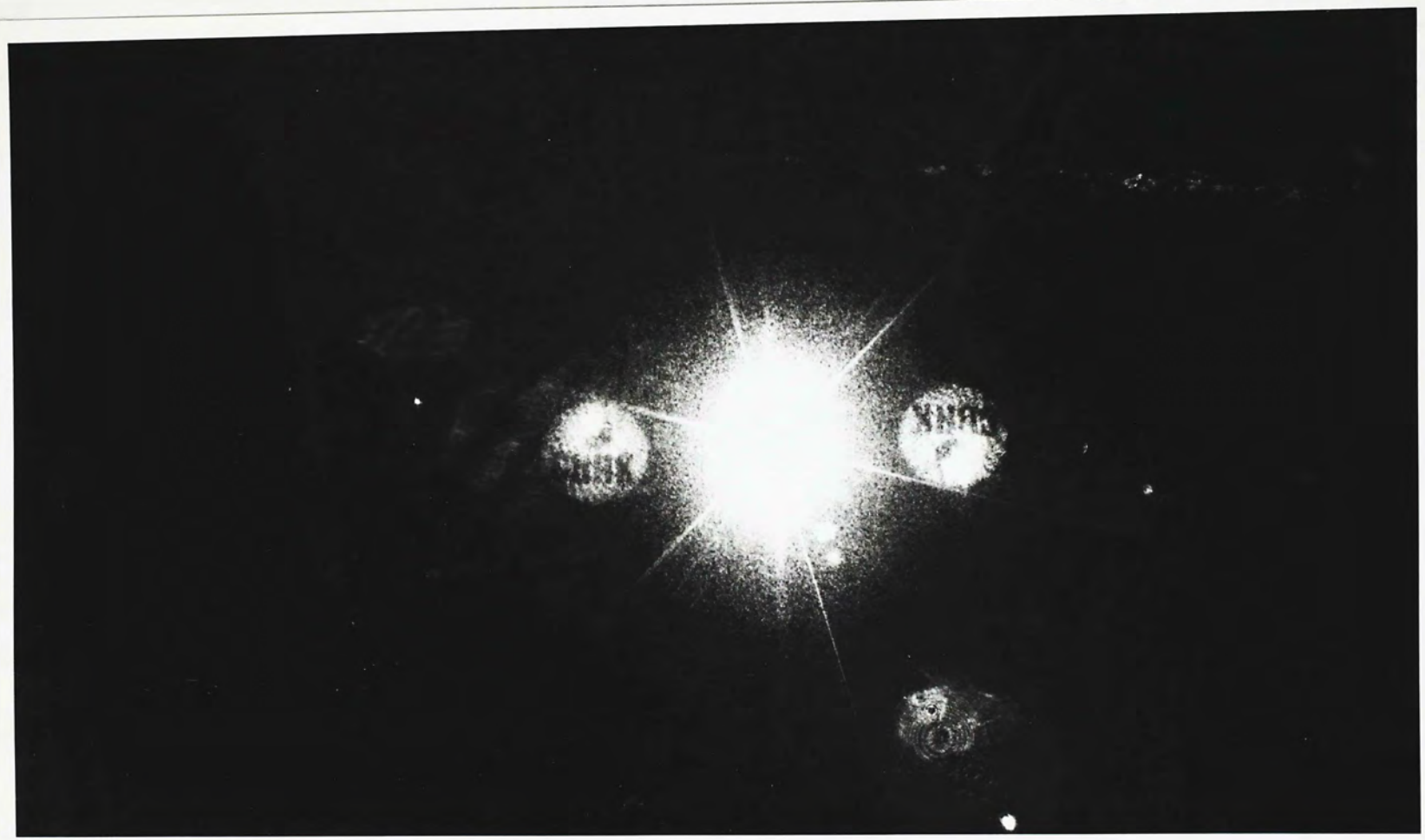

Fig. 4.7 Images reconstructed with linearly recorded three-beam interference lensless Fourier transform hologram with He-Ne laser beam

4.5 RECONSTRUCTION OF IMAGES FROM NONLINEARLY RECORDED THREE-BEAM INTERFERENCE LENSLESS FOURIER TRANSFORM HOLOGRAM WITH He-Ne LASER

The same hologram as that in Section 4.2 is used for reconstruction, but now the hologram is reconstructed with He-Ne laser beam with the optical configuration as shown in Fig. 3.8 .Photographs of reconstructed images are shown in Fig. 4.8 to Fig. 4.12 . Each photograph is focused on different diffraction orders to exhibit images on different diffraction orders.

The condition that not all images lie on the same image plane may be explained by the fact that the second reference point source is not in the subject plane.

All images located at zero to third diffraction orders are reconstructed, and the subject letters can be read out clearly in each diffraction order.

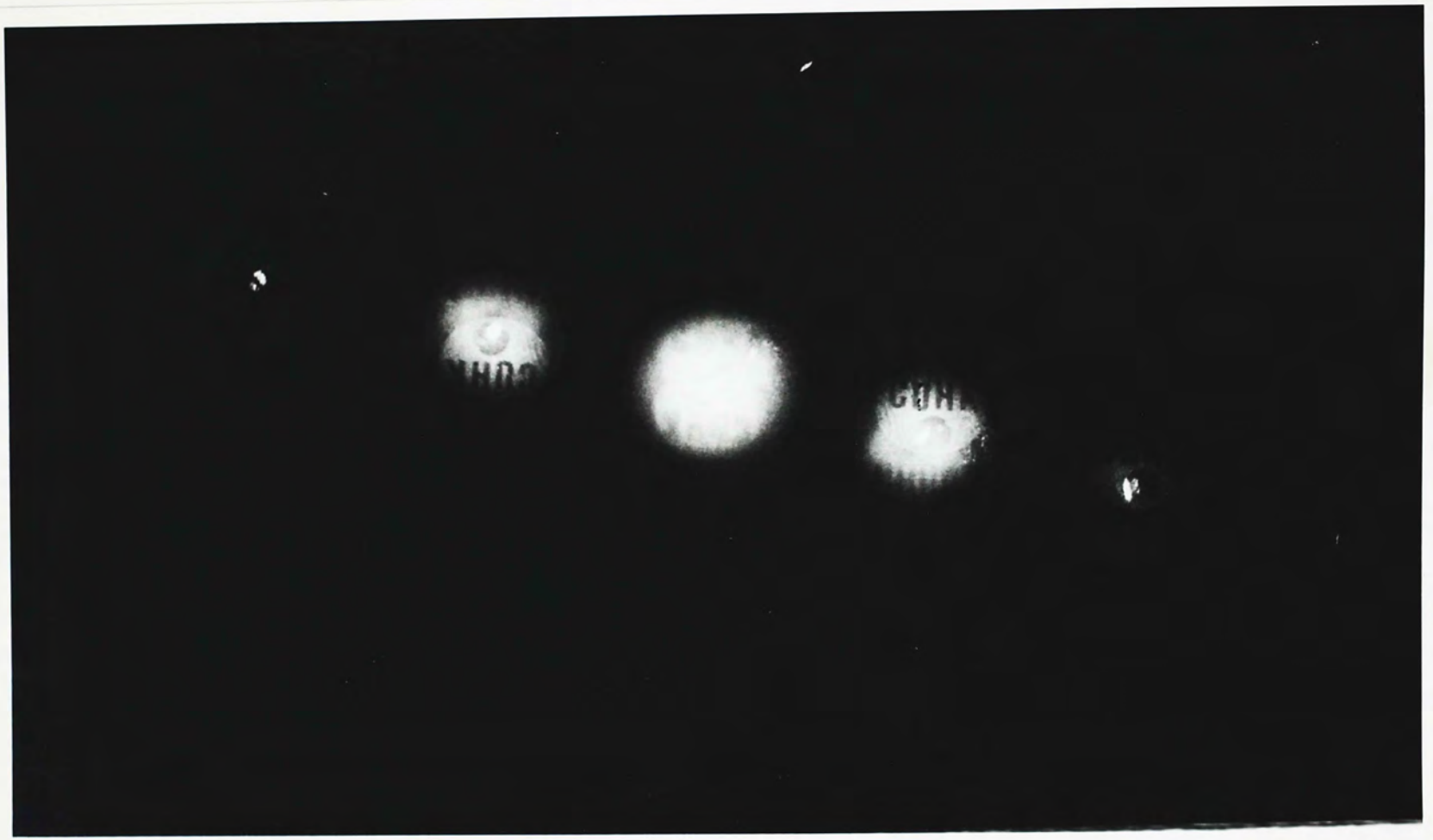

Fig. 4.8 Images reconstructed with nonlinearly recorded three-beam interference lensless Fourier transform hologram with He-Ne laser beam and focused on the central spot

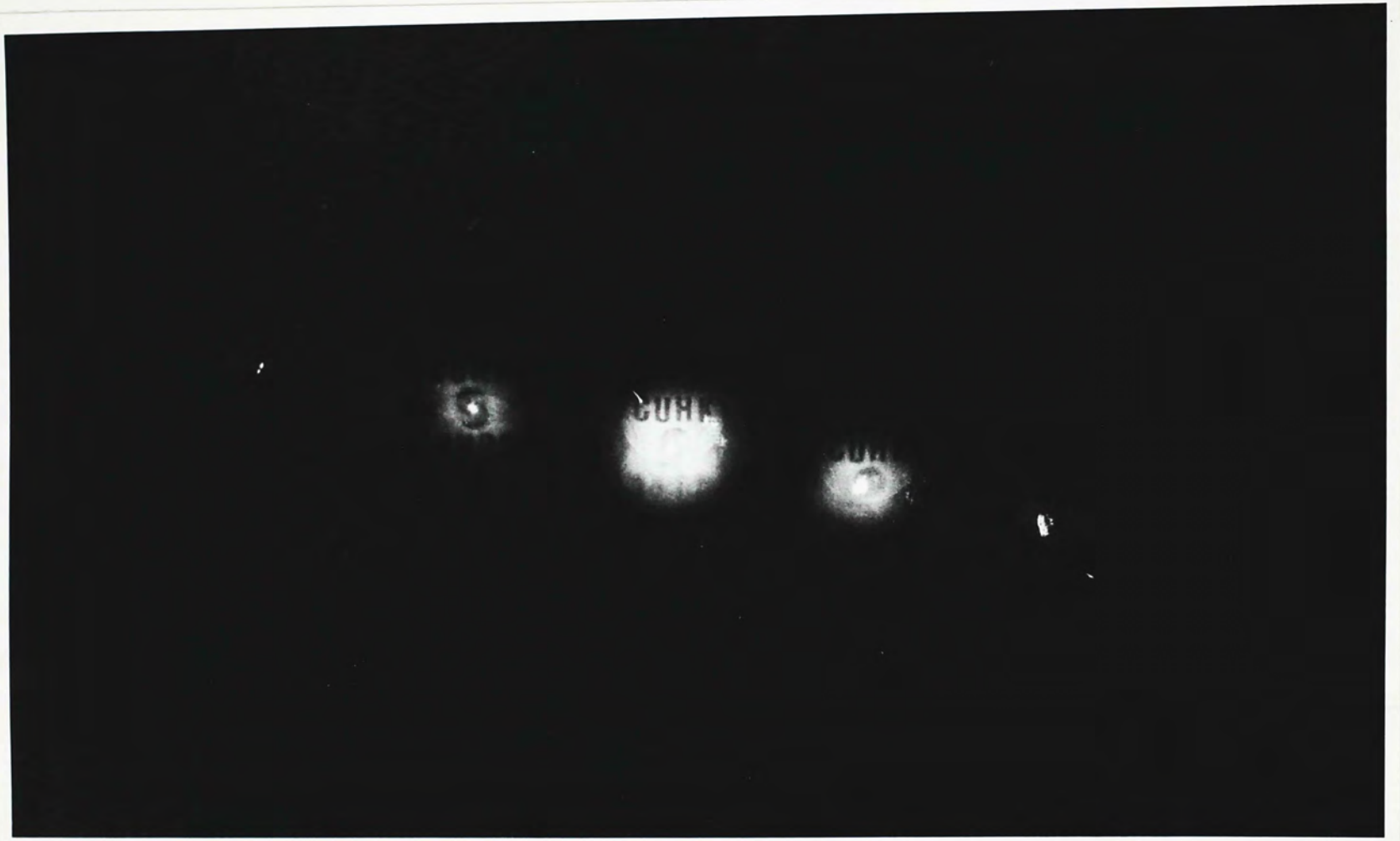

Fig.4.9 Images reconstructed with nonlinearly recorded three-beam interference lensless Fourier transform hologram with He-Ne laser and focused on the bright spot at +1 diffraction order

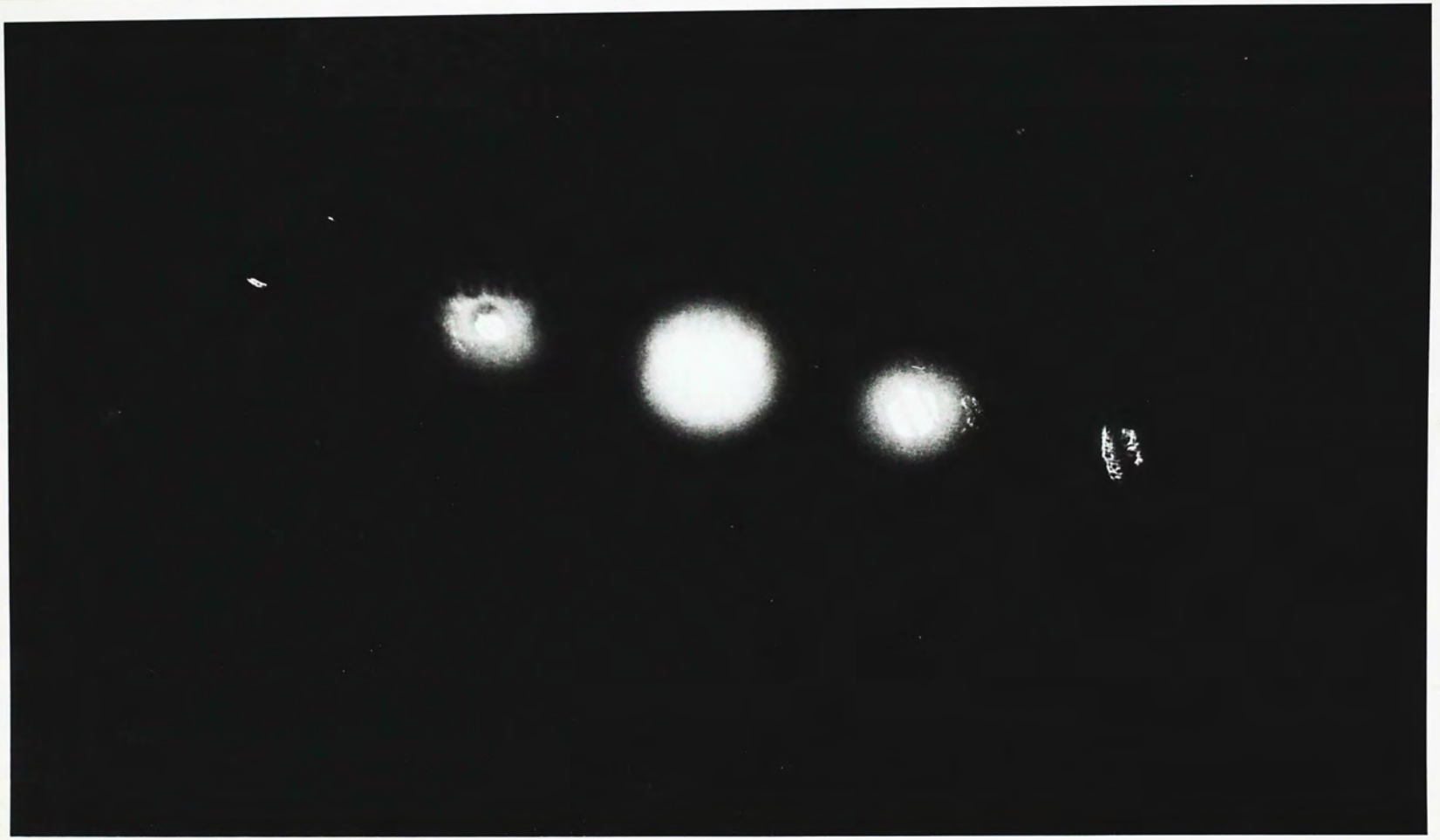

Fig.4.10 Images reconstructed with nonlinearly recorded three-beam interference lensless Fourier transform hologram with He-Ne laser and focused on the bright spot at +2 diffraction order

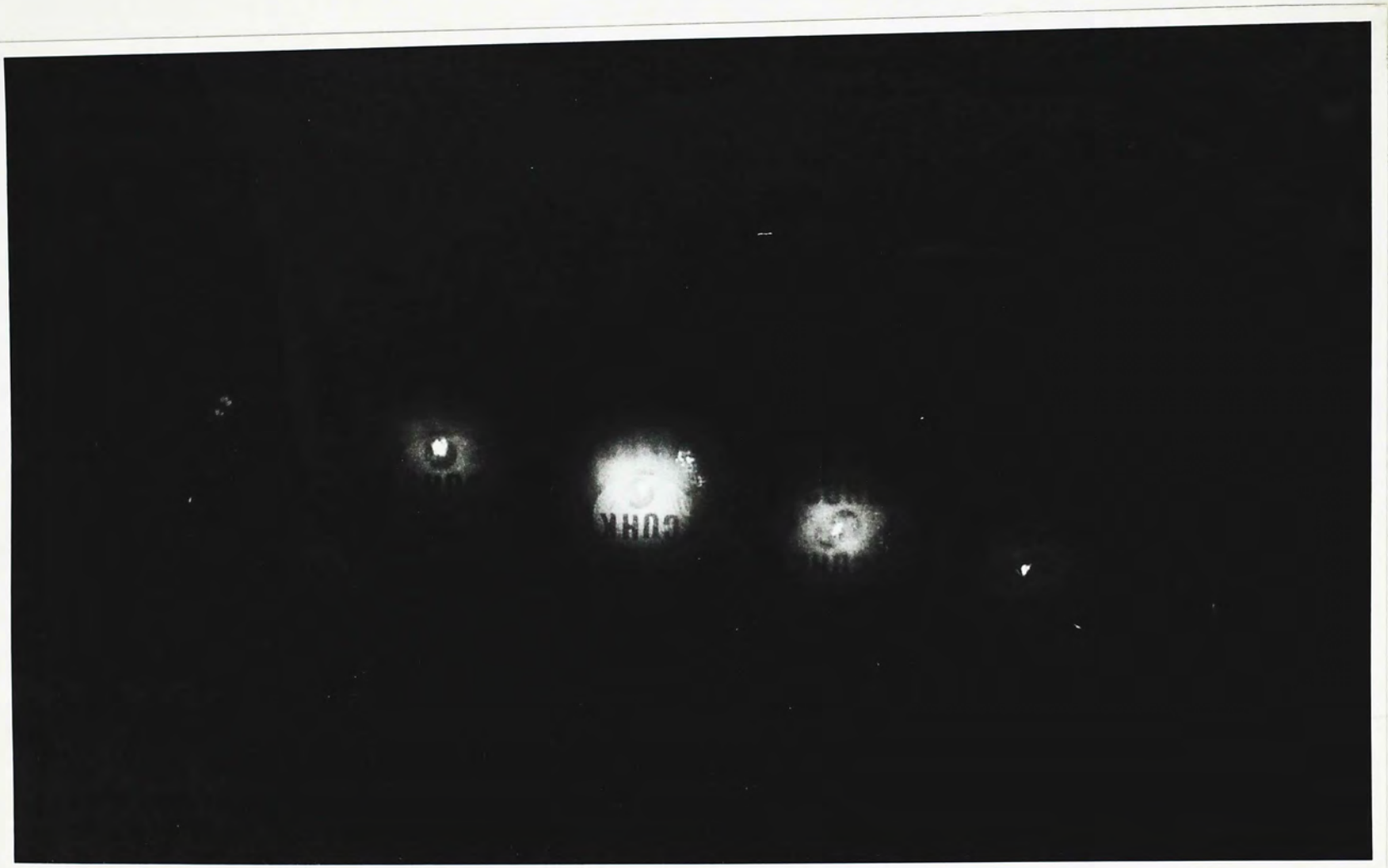

Fig.4.11 Images reconstructed with nonlinearly recorded three-beam interference lensless Fourier transform hologram with He-Ne laser and focused on the bright spot at -1 diffraction order

Fig.4.12 Images reconstructed with nonlinearly recorded three-beam interference lensless Fourier transform hologram with He-Ne laser and focused on the bright spot at -2 diffraction order

4.6 CONCLUSION AND DISCUSSION

The present work has shown that achromatic images can be acheived even with ordinary lensless Fourier transform holograms, and higher order images can be reconstructed if two reference beams are used in recording the hologram.

In this work, the second reference beam is introduced by making a hole underneath the subject letters. Achromatic images reconstructed by hologram made of interference of this second reference beam and the subject wave is shown in Fig. 4.1 and Fig. 4.2 . If a hologram is exposed for three-beam interference pattern, both images at the central zero-order position and the higher order images should be reconstructed simultaneously as theoretically predicted in Section 2.5 . However, the experimental result in Section 4.4 shows that the images at the location of central zero-order are still not observable as the 1st and 2nd order images are already reconstructed if the hologram is nonlinearly recorded. While both images located at the zero and higher orders are reconstructed simultaneously if the hologram is recorded nonlinearly as shown by the experimental result in Section 4.5 . These experimental results demonstrate the fact that with three-beam interference holograms, achromatic images are contributed mostly by the nonlinear effect. This is different from the linear effect with two-beam interference holograms.

If both reference sources are placed in the same plane in recording of the three-beam interference hologram, then no two images can be focused on the same plane in reconstruction with He-Ne laser. This result is expected for the same explanation given in Section 3.1 .

If the three-beam interference hologram is not recorded with

the arrangement of lensless Fourier transform but with that of Fresnel hologram, then two kinds of images will be reconstructed. The images reconstructed by the interference pattern of the subject beam and the second reference beam are Fourier transform images and achromatic. Interference of the subject beam and the first reference beam will give the ordinary 3-D images.

All the holograms in this work are bleached hologram with high diffraction efficiency. This bleaching process can bring about the higher order effect to the hologram. So an experiment is done to verify whether the achromatic images are due to higher order effect of bleaching process or nonlinear effect of overexposure. The experimental result shows that achromatic images can be reconstructed even with an unbleached hologram. Of course, intensity of the images reconstructed from an unbleached hologram is slightly weaker than that reconstructed from a bleached hologram, provided two holograms are recorded under exactly the same condition.

In this work, the incoherent light sources for reconstruction of achromatic images are a high pressure mercury vapour lamp or a high power projector. There is no difference in the reconstructed achromatic images. The only difference is the appearance in the color dispersion. Since Hg lamp gives a discrete spectrum while projector light source displays a continuous spectrum. Fig. 4.4 and Fig. 4.13 show the difference of reconstruction with Hg lamp and projector light source.

The next thing we want to emphasize is about the display of achromatic images with an additional grating. It is found that the recording of a grating with equal but opposite dispersion of the hologram

Fig.4.13 Achromatic image reconstructed with projector light source with nonlinearly recorded three-beam interference lensless Fourier transform hologram and focused on upper image

is not necessary. Gratings with fringe frequency equal to that of the hologram divided by an integral number can also be employed for dispersion compensation, e.g.

fringe frequency of the hologram = 150 fringes/mm.

fringe frequency of the grating = 78 fringes/mm.

Then the 1st diffraction order of the hologram is just diffracted back to zero-order by the 2nd diffraction order of the grating, and the viewer looks through the grating and hologram can observe an achromatic image. No gratings with fringe frequency greater than that of the hologram can be used for dispersion compensation.

The analysis in Chapter 2 propose that intensity of the three-beam interference pattern is given by

$$\begin{aligned} I &= (a+r+R)(a+r+R)^* \\ &= [\,a + (r+R)\,][\,a + (r+R)\,]^* \\ &= a^2 + (r+R)(r+R)^* + a(r+R)^* + a^*(r+R) \end{aligned} \qquad (4.1)$$

Now assume two two-beam interference holograms are made. The first hologram is a recording of the interference pattern of the subject wave and the first reference wave. Intensity of this interference pattern is given by

$$\begin{aligned} H &= (a+r)(a+r)^* \\ &= a^2 + r^2 + ar^* + a^*r \end{aligned}$$

The second hologram is a recording of the interference pattern of two reference beams. Intensity of this holographic grating is given by

$$G = (r+R)(r+R)^*$$

Then Eq. (4.1) can be rewritten in terms of H and G as

$$I = a^2 + G + a(r+R)^* + a^*(r+R)$$
$$= H + G - |r|^2 + aR^* + a^*R$$

The transmittance t of this three-beam interference hologram is given by

$$t \propto I = H + G - |r|^2 + aR^* + a^*R$$

if the hologram is linearly recorded.

If the hologram is nonlinearly recorded, then the hologram transmittance is proportional to sum of terms of higher order of I. Consider the quadratic effects only, transmittance of the nonlinearly recorded three-beam interference hologram is proportional to

$$I^2 = H^2 + G^2 + |r|^4 + (aR^*+a^*R)^2 + 2HG - 2H|r|^2 - 2G|r|^2$$
$$+ 2H(aR^*+a^*R) + 2G(aR^*+a^*R) - 2|r|^2(aR^*+a^*R) \qquad (4.2)$$

Reconstruction of this nonlinearly recorded hologram will give the images as shown in Fig. 2.8 . The only term we are interested in Eq. (4.2) is the fifth term, 2HG. This term is actually part of the total transmittance of the combination of two holograms recording the interference patterns of intensities H and G respectively, and it is this term, that is responible for the elimination of the color dispersion as demonstrated by Burckhardt [6]. An expression of HG in terms of a, r and R is given by

$$HG = K + 2r_o^2 ar^* + 2r_o^2 a^* r + (r_o^2+aa^*)r^*R + (r_o^2+aa^*)rR^*$$
$$+ a^*rrR^* + ar^*r^*R + a^*rr^*R + ar^*rR^* \qquad (4.3)$$

where $K = (2r_o^4 + 2aa^*r_o^2)$

Expressions of a, r, R are according to Eq.(2.2), Eq.(2.3) & Eq.(2.9). Images reconstructed by these two holograms combination is shown in Fig. 4.14. We can see that all the reconstructed images shown in Fig. 4.14 also appear in Fig. 2.8 .

The last two terms in Eq.(4.3) will give the achromatic images if the second reference source is displaced a small distance from the subject in recording of the holographic grating. If the subject is replaced by the second reference source in recording the holographic grating, then the achromatic images can be scarcely observed. The reason is due to the fact that the compensating grating will have opposite and equal dispersion to the hologram. If the second reference source is not displaced a small distance up or down from the subject, then the 1st order images diffracted back to the zero-order position by the holographic grating will just overlap with the central spot (D C portion of the reconstructed wave). Thus the subject cannot be read out for the high intensity of the central spot. Clear achromatic images will be observed if the second reference source is displaced up or down for a small distance. This condition is quite different from that reported in the previous experiments [6,7], in which ordinary transmission hologram is recorded and the holographic grating is formed by replacing the subject by the second reference source in exactly the same position. A Venetian blind is needed to place between the hologram and the compensating grating to block off the central spot and let through the diffracted wave. However, from experiment we know that this blocking must be at a large distance from the hologram. In fact, what we expect to observe with these two-beam interference holograms can also be

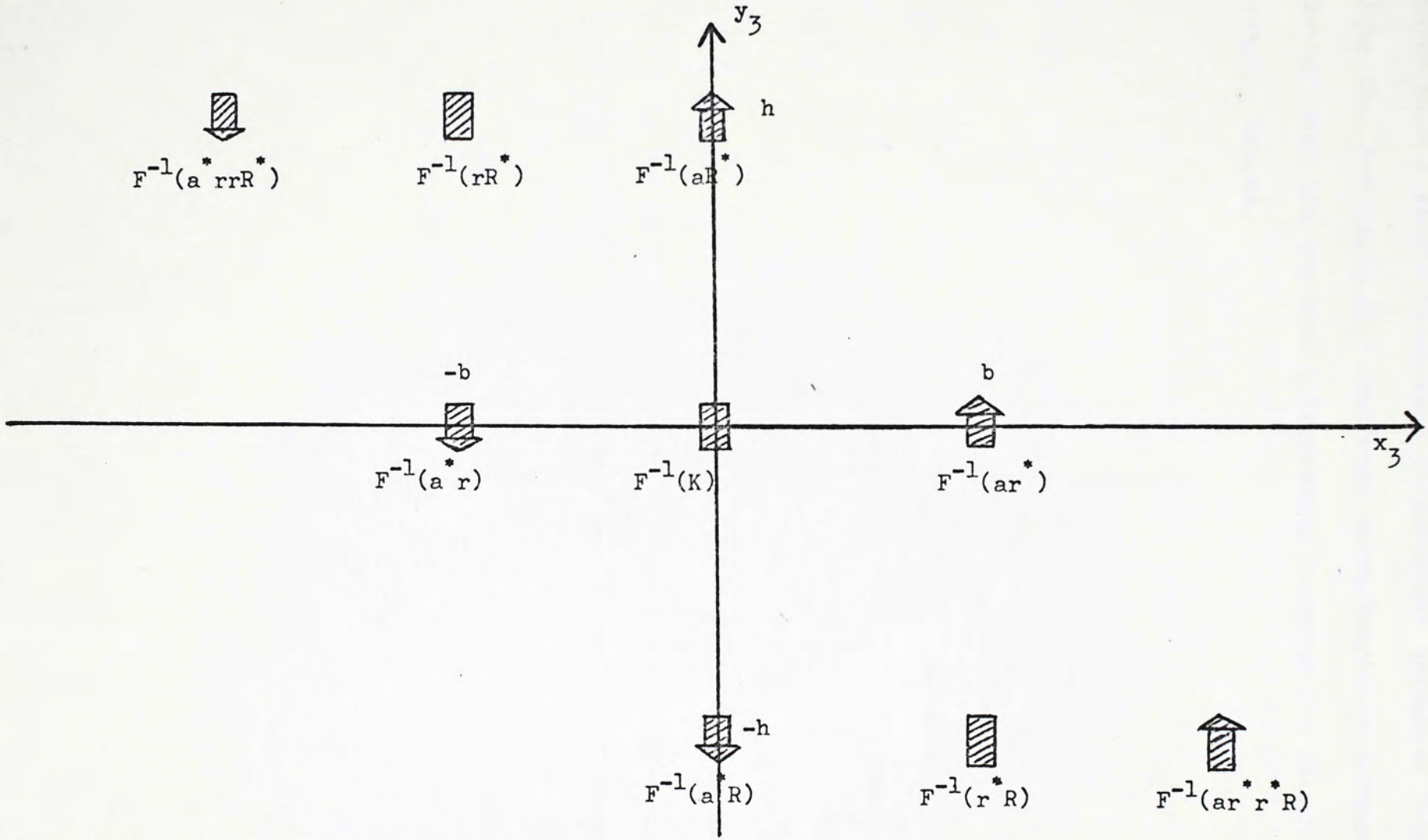

Fig. 4.14 Images reconstructed on the image plane with the combination of a two-beam interference lensless Fourier transform hologram and a holographic compensating grating

observed with a single three-beam interference hologram. Thus it is obvious that recording of a nonlinear three-beam interference hologram is better than two two-beam interference hologram for obtaining the achromatic images.

APPENDIX I

COHERENCE THEORY

Coherence effects are usually divided into two classifications, temporal and spatial coherence.

Temporal coherence relates directly to the finite bandwidth of the source. Temporal coherence is stated as the phase difference for two fixed points along a ray direction is time independent, or the difference in the phase measured at a single point in space at the beginning and end of a fixed time interval Δt does not change with time. Δt is called the coherence time, it is related to the bandwidth $\Delta \nu$ of the light source by

$$\Delta \nu \cong \frac{1}{\Delta t}$$

If the light is monochromatic, $\Delta \nu$ would be zero and Δt infinite. It is assumed that over interval much shorter than Δt, an actual wave behaves as if it were monochromatic. Thus Δt is the temporal interval over which the phase of the light wave at a given point in space can be reasonably predicted. Thus if Δt is large, the wave has a high degree of temporal coherence.

The distance for which one can just observe some degree of constancy of relative phase as a function of time, is a measure of the coherence length of the wave source. Coherence length ℓ is given by

$$\ell = c \, \Delta t$$

Spatial coherence relates to the finite extent of ordinary

light sources in space. Spatial coherence is stated as the phase difference for two fixed points in a plane normal to the ray direction is time independent.

If two laterally displaced points reside on the same wavefront at a given time, the fields at those points are said to be spatially coherent.

Suppose two apertures S_1 and S_2 are illuminated by an idealized point source S, then the wavelets issuing from S_1 and S_2 will remain a constant relative phase, they will be precisely correlated and therefore coherent. S_1 and S_2 are served as secondary sources and the wavelet emitted will be interfered and produce a stable fringe pattern. The field is said to be spatial coherent. On the contrast, if S_1 and S_2 are illuminated by separate thermal sources, no fringes will be observable since S_1 and S_2 have no correlation existed, then the fields at S_1 and S_2 are said to be incoherent.

Thus we find that the generation of interfence fringes is a very convenient and trustful measure of the coherence.

Interference and diffraction phenomena of electromagnetic waves are usually described with the aid of ideally coherent or ideally incoherent light beams. In the first case, the amplitudes of beams are superimposed and the superposition of such beams gives an observable interference pattern on the screen. In the second case, the intensities are superimposed and the interference pattern is not observable. However, real beams are correlated, such that they partially influence one another.

A superposition of such partially coherent light beams gives an

interference pattern whose visibility is less than the visibility of the interference pattern formed by coherent beams.

The main effect of partial coherence is that the depth of modulation of the intensity in the interference pattern is reduced, so that the minimum intensity no longer goes to zero.

The consequence for holography is reduced diffraction efficiency over the obtainable interference pattern with perfectly coherent light.

APPENDIX II

REFLECTION HOLOGRAM (LIPPMANN-BRAGG HOLOGRAM)

Reflection hologram is formed with the subject wave and reference wave illuminate opposite sides of the hologram plate as shown in Fig. II.1 .

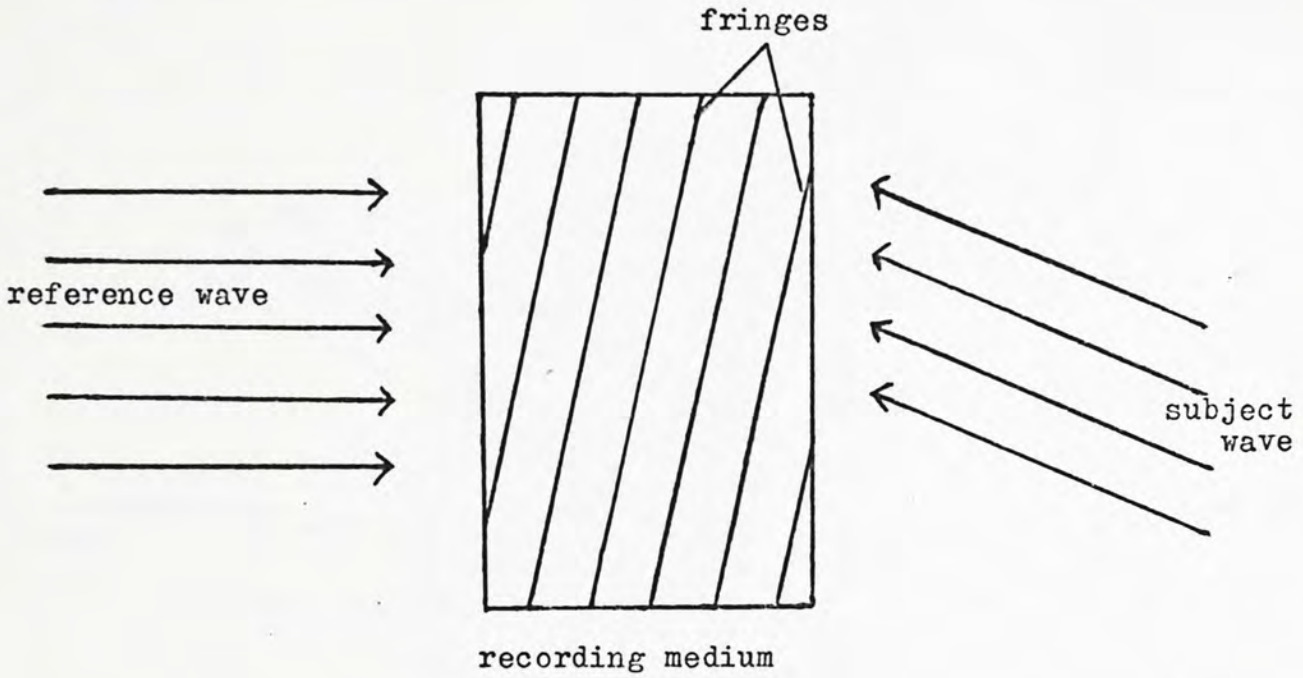

Fig. II.1 Formation of a reflection hologram

The interference of these two waves forms a stationary standing wave pattern in the recording medium. The fringes formed are approximately planes parallel to the surface of the hologram plate and separated by approximately half the wavelength in the recording medium. Since these fringe planes effectively form a helf-wave stack interference filter, readout may be accomplished with white light, as noted by Denisyuk [2], for in this case only a small band of wavelengths from the white light source satisfies the Bragg condition at one time. The Bragg condition requires that the angle of incidence equal the angle of diffraction and

at the same time both of these angles satisfy the grating equation. Violation of either of these conditions will limit the amount of light diffracted and the resulting image will not appear as bright as when the Bragg condition is fulfilled. Thus this kind of hologram is usually called Lipmann-Bragg hologram. The reconstructed image is viewed in reflection rather than transmission as shown in Fig. II. 2 .

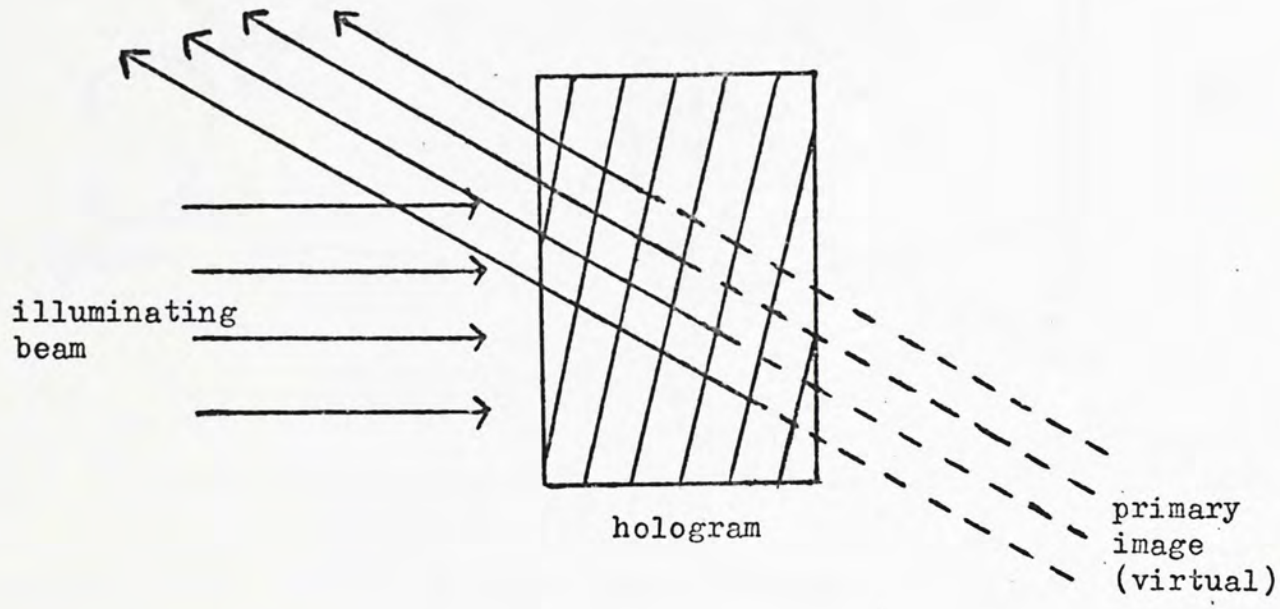

Fig. II. 2 Reconstructing the primary wave (virtual image) in reflection

This type of holograms has been proved experimentally and theoretically to be sufficiently to allow multicolor imaging with white light illumination [11, 12, 13].

APPENDIX III

FOCUSED-IMAGE HOLOGRAM

The image hologram is formed with the photographic plate lies in the central plane of the image formed by the lens as shown in Fig. III. 1 .

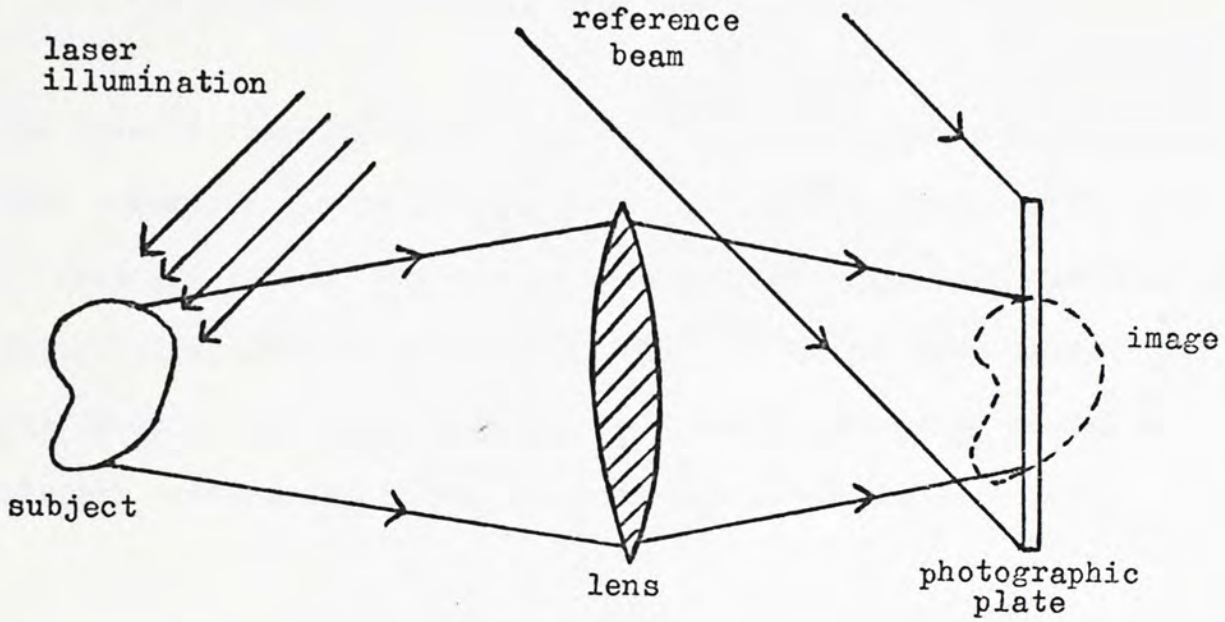

Fig. III. 1 Formation of an image hologram

Addition of the reference beam then allows formation of an image hologram. On reconstruction with the original reference wave, image hologram generates the same kind of images as those generated from lensless Fresnel holograms. However, the angle from which the image can be viewed is limited by the aperture of the lens and the 3-D image appears centred about the hologram plate. This kind of holograms has the merit of minimizing the requirements on the hologram illuminating source. It was proved that the minimum resolvable image dimension Δs [5] is given by

$$\Delta s = \left(\frac{z_1}{z_r} \right) \Delta r$$

where Δr = extent of source which describes the degree of spatial coherence of the illuminating source

z_1 = distance of image from the hologram

z_r = distance of source from the hologram

In the case of image hologram, $z_1 \rightarrow 0$, even large sources with little spatial coherence can be used to generate hologram images with sufficient resolution. The consequence is that image holograms can be brightly illuminated by extended source [3]. It was also proved that [5] displacement of the image position when the illuminating source of wavelength difference $\Delta\lambda$ from one original reference wave is

$$\Delta\sigma = \theta_r \, z_1 \left(\frac{\Delta\lambda}{\lambda} \right)$$

where θ_r = angle which the reference beam makes with the normal to the hologram plane

λ = the central wavelength of the illuminating source

When both θ_r and z_1 are small, the illuminating source bandwidth may be large and yet have small effect on the minimum resolvable image spot. Thus the image resolution in the hologram plane is unaffected by the spread in wavelength of the illuminating light.

When white light source is used in reconstruction, all wavelength components of white light illuminating such image holograms are equally well focused to image points on the hologram plane, then the central plane of the image, located on the hologram will then

appear achromatic. However, for image points out of the hologram plane, color dispersion and blurring which degrade the resolution becomes noticeable to a degree determined by the offset angle of the reference beam and the distance of the points from the hologram plane.

The three-dimensional images can also be reconstructed by transmission of white light through a hologram recorded in a special arrangement using an 'in-line' coherent background superposed onto a conventionally focused image field [14].

This experimental process was first called " Focused Image Holography" by Stroke [15] and provides a method for restoring the third dimension in the recording of conventionally Focused Photographs[16].

APPENDIX IV

RECORDING WITH UNFILTERED MERCURY ARC

The basic idea in making incoherent hologram is to have each point in the subject form its own reference beam. This can be accomplished by splitting the wavefront from each point in the subject and causing the two resulting wavefronts to interfere in such a way as to form its own interference pattern. The hologram then consists of the incoherent addition of the interference patterns originating from all points of the subject. In fact, noncoherence between the various subject points is a requirement for holography with noncoherent light. Later, each interference pattern reconstructs its own subject point in the reconstruction process and hence an image is produced.

Experiments on hologram making using incoherent mercury light source were done and the images were reconstructed with coherent light beam from He-Ne laser [28-31]. However, an interference filter is usually added so that only light waves of narrow bandwidth centred at 5461A mercury green line is used in recording the hologram. Thus the light source in recording is practically monochromatic.

With reference to the work of B.J. Chang [35], it is believed that incoherent holograms can also be recorded with the whole discrete spectrum of mercury. Thus this experiment is devoted to the study of incoherent holograms with unfiltered mercury arc.

This experiment is also based on the above theory with some modifications. The experimental set up is shown in Fig. IV. 1 .

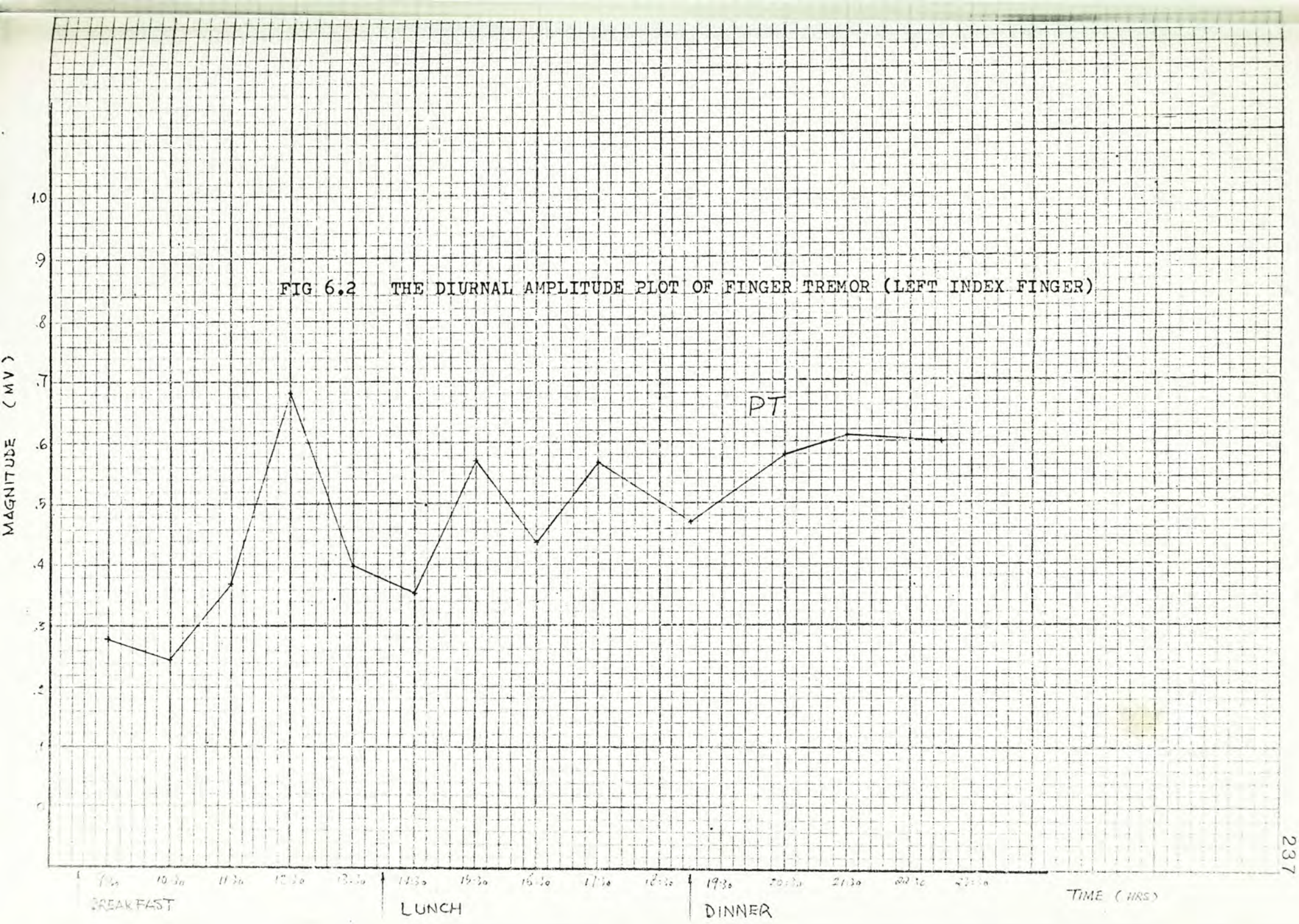
FIG 6.2 THE DIURNAL AMPLITUDE PLOT OF FINGER TREMOR (LEFT INDEX FINGER)
MAGNITUDE (MV)
1.0
.9
.8
.7
.6
.5
.4
.3
PT
BREAKFAST
LUNCH
DINNER
TIME (HRS)

The Michaelson Interferometer is employed as a beam splitter to split the incident light beam from the mercury arc into two. Then for each point in the subject beam, there is a corresponding point in the reference beam so that wavefronts from this pair of corresponding points are coherent.

A transparent letter F on a large balck background is used as the subject. This subject transparency is placed in the optical path of one beam and slightly diffused image of the subject letter is projected on the photographic plate. The other light beam which directly illuminates the photographic plate is acting as the reference beam. Wavefronts from each pair of corresponding points in the subject transparency and the reference beam form its own interference-fringe grating on the photographic plate. Location of the photographic plate is adjusted so that the subject and reference beams interfere on the photographic plate and high contrast interference fringes are focused onto this plane.

After the normal dark room processing as stated in Section 3.2, images are reconstructed with He-Ne laser as the illuminating source.

Experimental set up for reconstruction is shown in Fig. IV.2. The divergence lens is used to expand the laser beam, whilst the positive lens L_1 and L_2 are used to resemble the original reference beam. The image plane is slightly behind the focal plane of the combined lens system. As the subject is placed slightly before the focal plane of the positive lens (f = +350mm) in recording, real images are expected on a plane slightly behind the focal plane of the positive lens L_2 in reconstruction.

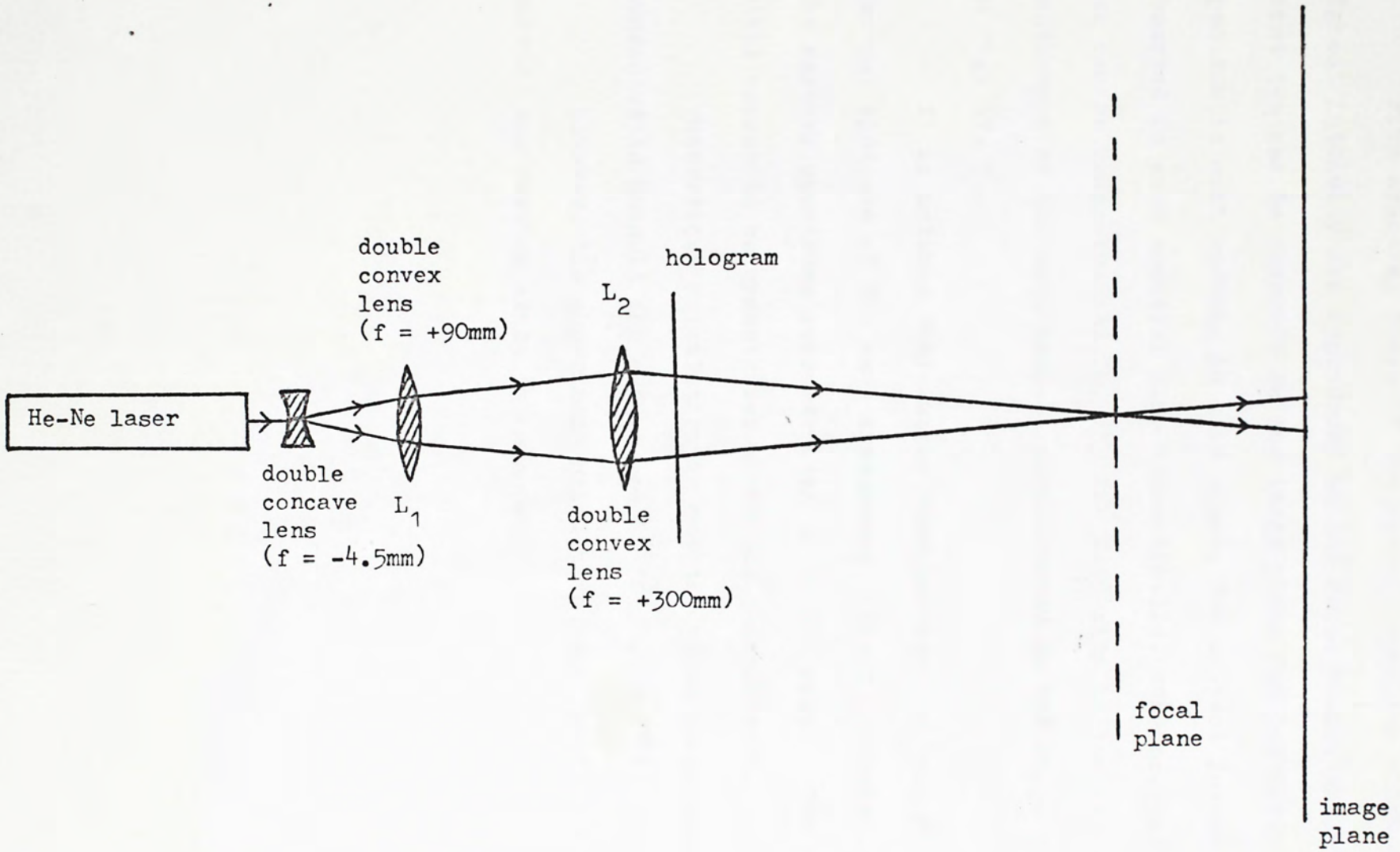

Fig. IV.2 Experimental set up for reconstruction with incoherent holograms

Five spectral lines of the mercury spectrum which are of highest intensity are reproduced on the focal plane, whilst only the first two can be observed on the image plane for intensity of the spectrum is much reduced in this plane. The subject letter should be observed in each spectral line theoretically. However, only the first two can be reconstructed for the low intensity in the image plane. Photograph of the real images reconstructed on the image plane is shown in Fig. IV. 3 .

It is noticed that images reconstructed on both sides of the central spot are of the same appearance without inversion. Of course, the mercury spectrums reconstructed on either side of the central spot still appear to be symmetrized about the central spot.

Theoretical calculation is not discussed here. Readers are suggested to consult the references [36,37] .

However, the experiment still have many problems needed to be solved, and further study is necessary.

Fig.IV.3 Real images reconstructed on the image plane with an incoherent hologram illuminated by He-Ne laser

APPENDIX V

FRESNEL-KIRCHHOFF INTEGRAL

If a plane wave of amplitude a_1 , travelling in the direction of the positive z-axis, is incident on an subject with amplitude transmittance $s(x_1,y_1)$ in the plane normal to the z-axis at z=0 , the light complex amplitude $a_2(x_2,y_2,d)$, in the plane z=d is

$$a_2(x_2,y_2,d) = \frac{ia_1}{\lambda} \int_{x_1=-\infty}^{\infty} \int_{y_1=-\infty}^{\infty} s(x_1,y_1) \times \exp \frac{\left\{-i \frac{2\pi}{\lambda} [d^2+(x_2-x_1)^2+(y_2-y_1)^2]^{\frac{1}{2}}\right\}}{[d^2+(x_2-x_1)^2+(y_2-y_1)^2]} \cos\theta \, dx_1 dy_1$$

The angle θ is formed by the positive z-axis and the straight line connecting the points $(x_1,y_1,0)$ and (x_2,y_2,d) . $\cos\theta$ is called the obliquity factor.

A derivation of the Fresnel-Kirchhoff integral can be found in O'Neill [23] or Born & Wolf [24] .

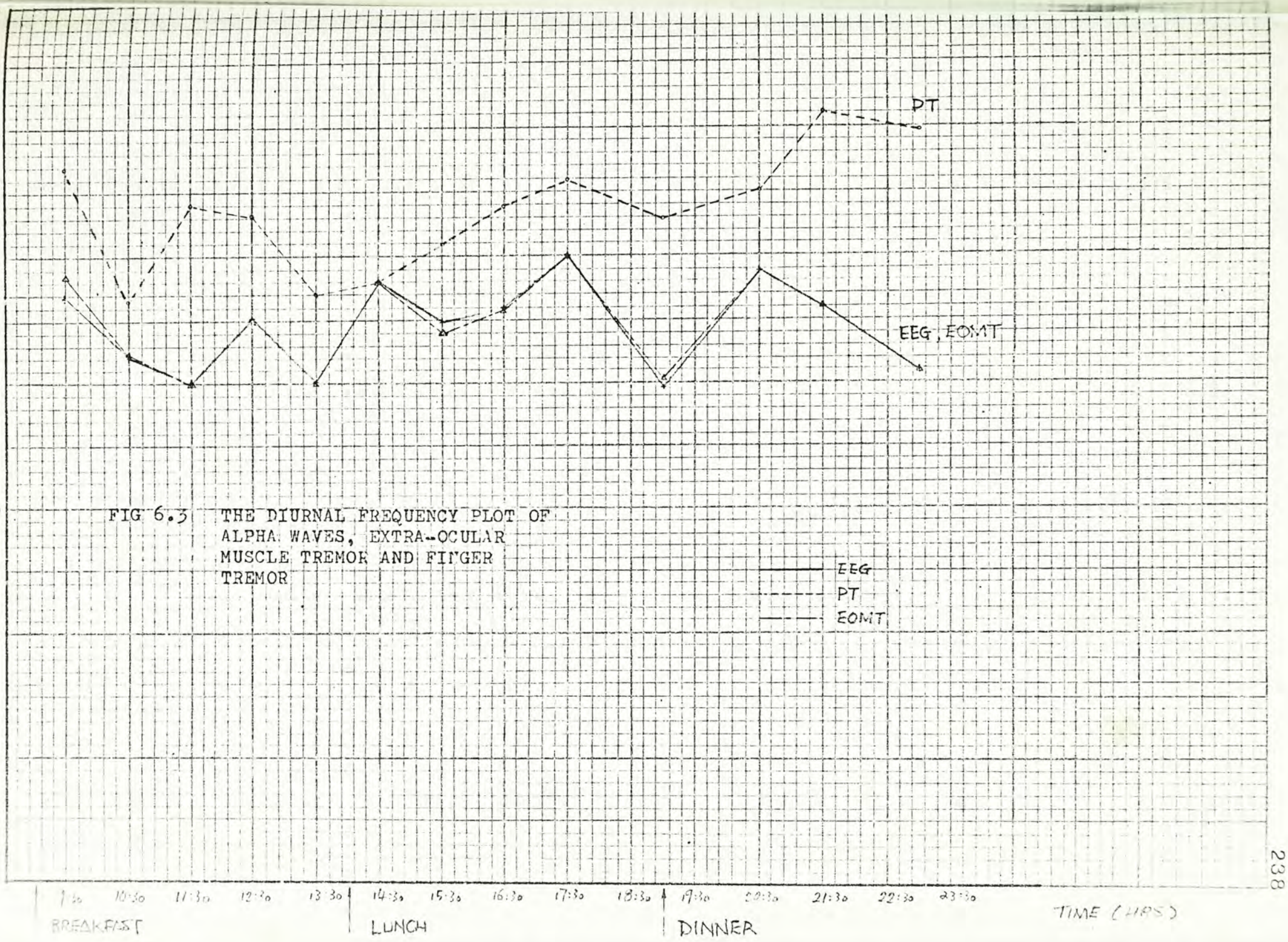

FIG 6.3 THE DIURNAL FREQUENCY PLOT OF ALPHA WAVES, EXTRA-OCULAR MUSCLE TREMOR AND FINGER TREMOR

APPENDIX VI

THE t-E CURVE FOR KODAK 649F EMULSION

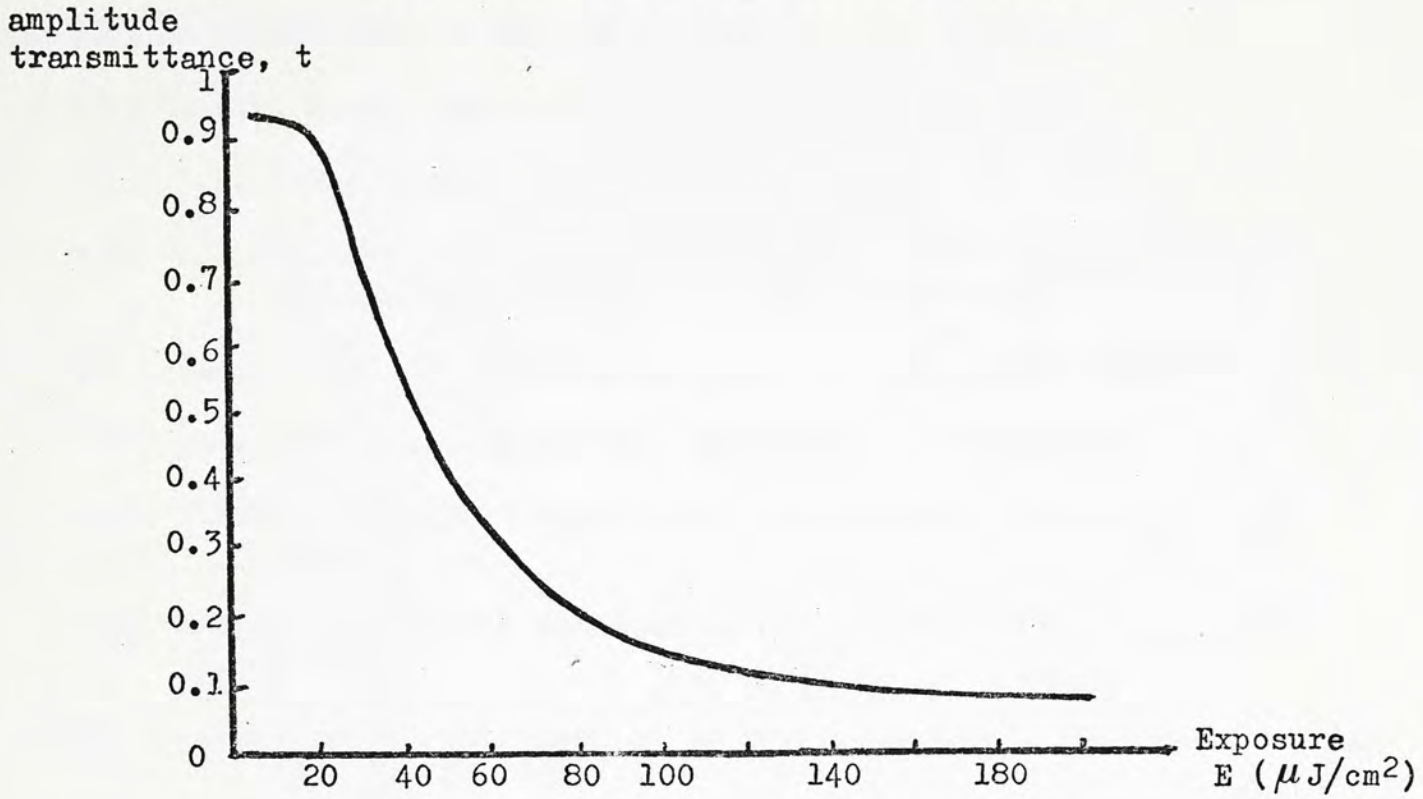

The process of developing the hologram is one of the factors determining the shape of the curves, but the form of curve does not depend strongly on the wavelength. Change of the wavelength merely change the horizontal scale of exposure E in accord with the spectral sensitivity of photographic emulsion for different wavelength [25].

If the range of exposure is kept withing the portion of the t-E curve which is approximately linear, the transmittance t is given by

$$t = t_o - KI$$

If the range of exposure fall out the linear portion, the transmittance is given by

$$t = c_o + c_1 I + c_2 I^2 + c_3 I^3$$

REFERENCE

[1] G.W. Stroke and A.E. Labeyrie, Phys. Letters, 20 , 368 (1966)

[2] Y.N. Denisyuk, Soviet Phys. Doklady, 7 , 543 (1962)

[3] Lowell Rosen, Appl. Phys. Letters, 9 , 337 (1966)

[4] G.B. Brandt, Appl. Opt., 8 , 1421 (1969)

[5] R.J. Collier, C.B. Burckhardt and L.H. Lin, Optical Holography, (Academic Press 1971) 1st ed., p. 204-206

[6] C.B. Burckhardt, Bell Syst. Tech. J., 45 , 1841 (1966)

[7] D.J. DeBitetto, Appl. Phys. Letters, 9 , 417 (1966)

[8] Yasukiro Torii and Masao Sumi, Jap. J. Appl. Phys., 11 , 644 (1972)

[9] Yasuhiro Torii and Masao Sumi, Jap. J. Appl. Phys., 11 , 1308 (1972)

[10] J.W. Goodman, Introduction to Fourier Optics , (McGraw-Hill 1968) 1st ed., p.240-242

[11] L.H.Lin, K.S. Pennington, G.W. Stroke and A.E. Labeyrie, Bell Syst. Tech. J., 45 , 659 (1966)

[12] J. Upatnieks, J. Marks and R.J. Fedorowicz, Appl. Phys. Letters, 8 , 286 (1966)

[13] L.H. Lin and C.V. LoBianco, Appl. Opt., 6 , 1255 (1967)

[14] G.W. Stroke, Phys. Letters, 23 , 325 (1966)

[15] Lowell Rosen, Proc. IEEE, 55 , 79 (1967)

[16] W.E. Kock, L.Rosen and G.W. Stroke, Proc. IEEE, 55 , 80 (1967)

[17] A.R. Shulman, Optical Data Processing, (John Wiley & Sons, Inc. 1970) p. 482-495

[18] R.J. Collier, C.B. Burckhardt and L.H. Lin, Optical Holography, (Academic Press, 1971) p.280-283

[19] S.T. Hsue , Private communication

[20] J. Upatnieks and C. Leonard, Appl. Opt., 8 , 85 (1969)

[21] Processing Chemicals and Formulas for black and white Photography, (Eastman Kodak Company, 1970) 6th ed.

[22] Kodak Plates and Film for Science and Industry, (Eastman Kodak Company, 1967)

[23] E.L. O'Neill, Introduction to Statistical Optics, (Addison-Wesley, 1963) p.72ff

[24] M. Born and E. Wolf, Principles of Optics, (Pergamon Press, 1970) 4th ed., p.378-382

[25] R.J. Collier, C.B. Burckhardt and L.H. Lin, Optical Holography, (Academic Press, 1971) 1st ed., p.282-284

[26] A.W. Lohmann, J. Opt. Soc. Am., 55 , 1555 (1965)

[27] G.W. Stroke and R.C. Restrick III, Appl. Phys. Letters, 7 , 229 (1965)

[28] G.D. Cochran, J. Opt. Soc. Am., 55 , 615 (1965)

[29] C.R. Worthington, J. Opt. Soc. Am., 56 , 1397 (1966)

[30] G.D. Cochran, J. Opt. Soc. Am., 56 , 1513 (1966)

[31] P.J. Peters, Appl. Phy. Letters, 8 , 209 (1966)

[32] O. Bryngdahl and A. Cohmann, J. Opt. Soc. Am., 58 , 625 (1968)

[33] R.H. Katyl, Appl. Opt., 11, 1241, 1248 and 1255 (1972)

[34] E.N. Leith and B.J. Chang, Appl. Opt., 12 , 1957 (1973)

[35] B.J. Chang, Opt. Commun., 9 , 357 (1973)

[36] G.W. Stroke, An Introduction to Coherent Optics and Holography, (Academic Press, 1969) 2nd ed., Chapter 3

[37] M. Born & E. Wolf, Principles of Optics , (Peigamon Press, 1970) 4th ed., Chapter 10